DOKUZ EYLÜL UNIVERSITY
GRADUATE SCHOOL OF NATURAL AND APPLIED SCIENCES

DESIGN AND EVALUATION OF A HYBRID PASSIVE/ACTIVE RIPPLE FILTER

by
Emre AYĞIN

November, 2006
İZMİR

DESIGN AND EVALUATION OF A HYBRID PASSIVE/ACTIVE RIPPLE FILTER

A Thesis Submitted to the
Graduate School of Natural and Applied Sciences of
Dokuz Eylül University
In Partial Fulfillment of the Requirements for
the Degree of Master of Sience in Electrical and Electronics Engineering ,

by
Emre AYĞIN

November, 2006
İZMİR

M.Sc THESIS EXAMINATION RESULT FORM

We have read the thesis entitled **"DESIGN AND EVALUATION OF A HYBRID PASSIVE/ACTIVE RIPPLE FILTER"** completed by **Emre AYĞIN** under supervision of **Prof. Dr. Haldun KARACA** and we certify that in our opinion it is fully adequate, in scope and in quality, as a thesis for the degree of Master of Science.

.....

Prof. Dr. Haldun KARACA
(Supervisor)

.....

(Jury Member)

.....

(Jury Member)

Prof.Dr. Cahit HELVACI
Director
Graduate School of Natural and Applied Sciences

ACKNOWLEDGMENTS

I would like to thank my supervisor Prof. Dr. Haldun KARACA for his valuable guidance and support during the course of this thesis.

Finally, I owe the nearest standing me my deepest gratitude, especially my family, for understanding and encouragement throughout this work.

Emre AYĞIN

DESIGN AND EVALUATION OF A HYBRID PASSIVE/ACTIVE RIPPLE FILTER

ABSTRACT

Active ripple filters can substantially attenuate power converter ripple, allowing considerable reduction in passive filter component size. Investigated here is a hybrid passive/active filter topology that achieves ripple reduction by injecting a compensating voltage ripple across a series filter element. Input and output filters have become an extremely important part of modern switching power converters, and often account for a substantial portion of converter size and cost. Traditionally, passive LC low-pass filters have been employed to attenuate power converter switching ripple to acceptable levels.

This paper explores the design of hybrid passive/active filter topology that achives ripple reduction by injecting a compemsating voltage ripple across a series fitler element and current ripple cancellation, including the design tradeoffs, advantages, and limitations of different implementation methods.

Keywords : Hybrid passive/active filter, switching ripple, ripple attenuation.

HİBRİT/PASİF , AKTİF FİLTRELERİN İNCELENMESİ VE TASARIMI

ÖZ

Hibrit aktif / pasif filtreler anahtarlamalı güç dönüştürücülerindeki çıkış gerilim dalgalanmalarını önemli ölçüde azaltır. Burada seri filtre elemanları gerilim dalgalanmalarını içine atarak söz konusu dalgalanmaları azaltmayı başaran hibrid pasif ve aktif filtreleri incelenmiştir. Giriş ve çıkış filtreleri modern anahtarlayıcı güç dönüştürücülerin çok önemli bir parçası olmuştur ve dönüştürücünün büyüklüğü ve maliyeti açısından hesaba katılır.

Bu tezde, seri filtre elemanlarına karşı ve akım dalgalanmalarını azaltan, ve farklı uygulama metotlarını sınırlandıran, gerilim dalgalanmalarını içine atarak bunları azaltmayı başaran aktif ve pasif filtre topolojilerin değerlendirmesi yapılmıştır.

Anahtar sözcükler : Hibrit pasif/aktif filtreleri, rezonant boşalımları

CONTENTS

Page

CHAPTER ONE
INTRODUCTION

In telecommunications and computing systems, the continuous trend in miniaturizing power processing subsystems, which are in charge of guaranteeing high efficiency in the use of supply energy, stands from the global system-level impact of those subsystems in terms of volume and weight, and thus on portability. This statement is particularly true for actual and future generation systems-on-chip, a trend which provides a line of convergence for the implementation of current and future systems for low-power portable, mobile and autonomous applications, in which power management is one of the key performance limiting factors as regards to ergonomics and operability time. The ultimate target consequently consists in the fully monolithic integration of the power converter together with the same circuits which constitute its load within either the same substrate or chip package, yielding a complete Powered System on a Chip. Despite the notable research efforts in the field of integrated switching power converters, further investigations are required to achieve further miniaturization and better efficiency while retaining compatibility with an integrated technology, in particular with digital CMOS technology, the standard technology for signal processing and computation and the target for RF IC implementations. In the investigation towards full-integration of switching power converters, research both on optimized converter topologies, active devices, integrable passive elements and controller circuits is required.

Input and output filters have become an extremely important part of modern switching power converters, and often account for a substantial portion of converter size and cost. Reliable and precise filtering of dc supplies, for example on spacecrafts is an important consideration in establishing the overall integrity of a space power system. Since the primary source of electrical power on most spacecraft is a widely fluctuating direct voltage, dc-to-dc converters are employed to provide the various regulated dc supply voltages. These converters commonly operate at switching frequencies in the range of 2-50 kHz and require output filters with nondissipative dc current paths. L-section or pure-capacitance filters which use large amounts of

capacitance are commonly employed with converters to provide the smooth dc supply voltages. These dc filter capacitors for satellite static power-converter applications have long been a problem. It is not only because of the bulky size required to provide the needed microfarads but also because of their relatively low reliability in the environment of outer space. Among the many different types of capacitors currently available, tantalum electrolytic capacitors are the most widely used due to their large capacitance per unit volume. Some other types of capacitors such as ceramic or mica have better reliability but have much smaller capacitance per unit volume. Therefore, if the required filter capacitance can be reduced, even by increasing circuit complexity, so that more reliable capacitors such as ceramic or mica can be used, the overall filter reliability may be increased. Various techniques for capacitance reduction are currently available. However, they generally do not have dc current paths or they have dissipative elements in the dc current paths. By employing properly designed magnetically coupled circuits, the ripple niters presented in this paper have the potential to utilize the more reliable small-microfarad capacitors, provide non-dissipative dc current paths, and achieve approximately the same response as the existing L-section or pure-capacitance filters. For these reasons, they would appear to have advantage also when applied to dc power supplies other than for space application.

Two configurations of ripple filters, one passive and one active, used to filter the output ripple of dc-to-dc converters and other power supplies are discussed. The passive one uses a small-microfarad capacitor and a mutual inductor; the active one uses these same components and, in addition, an operational amplifier. These filters have potential for most of the applications to enable the designer to use more reliable types of capacitors such as ceramic or mica instead of tantalum capacitors now commonly used in the conventional L-section or pure-capacitance filters requiring large-microfarad capacitance. The passive filter has achieved attenuation greater than 40 dB and the active filter greater than 50 dB. Both of these filters accomplished significant capacitance reduction when compared with an L-section filter for the same application.

Traditionally, passive LC low-pass filters have been employed to attenuate power converter switching ripple to acceptable levels. However, the tight ripple specifications that are often imposed for application reasons or to meet conducted EMI (Electromagnetic interference) specifications can result in bulky and expensive filters which are detrimental to the transient performance of the system. This is especially true for systems which operate at low voltage and/or high current levels, due to the nature of the filter components and their parasitics.

An alternative to the conventional approach is the use of an active ripple filter, in which an active electronic circuit (typically coupled with a reduced passive filter) is used to cancel or suppress ripple components at the filter output. Typically, the reduced passive filter attenuates the ripple to an intermediate level at which the active electronics can cancel or suppress the ripple to an even lower level without undue power loss. For example, a feedforward active ripple filter can be used in conjunction with a passive filter at the output of a buck converter. The active filter senses the ripple current in the passive filter inductance and shunts an exact copy of it away from the output capacitance and load. This reduces the ripple seen at the output, and permits a substantially smaller passive filter to be employed than would otherwise be possible. Potential benefits of the active filter approach thus include reduction of the converter size and cost, and improvements in transient performance.

Many types of active ripple filters are possible. Ripple-current filters reduce the ripple current passing through a circuit branch, while ripple-voltage filters reduce the voltage ripple at a node. Feedforward filters achieve the ripple reduction by measuring a ripple component and injecting its inverse, while feedback filters operate to suppress the ripple via high-gain feedback control. Hybrids of these filter types are also possible, and active filters maybe further classified by how the sensing and driving functions are implemented.

CHAPTER TWO
PASSIVE FILTER DESIGN

Today, almost all modern equipment uses some kind of power supply. There are a lot of different circuit topologies used. All power circuits conditioning requires some kind of an input filter. The input LC filter has become very critical in its design and must be designed not only for EMI, but also for system stability, and for the amount of ac ripple current drawn from the source (Silber, 1975).

The input voltage supplied to the equipment is also supplied to other users. For this reason, there is a specification requirement regarding the amount of ripple current seen at the source, as shown in Figure 2.1. Ripple currents generated by the user induce a ripple voltage, Vz, across the source impedance. This ripple voltage could impede the performance of other equipment connected to the same bus.

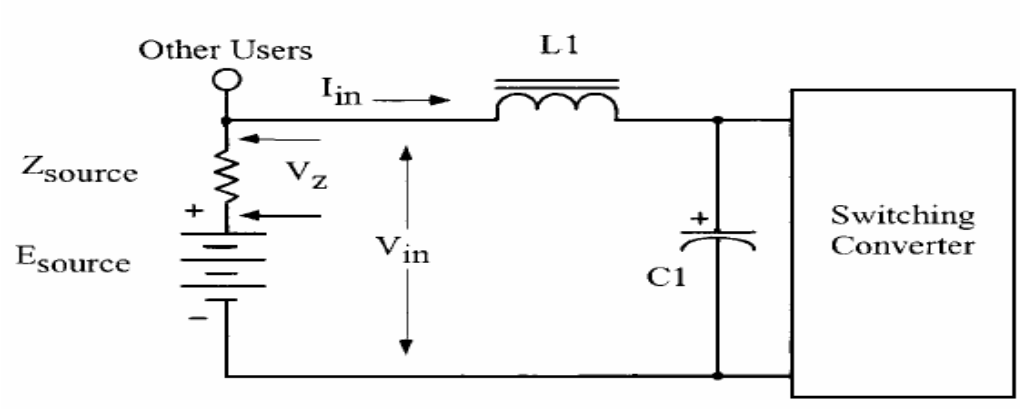

Figure 2.1 Simple LC Input Filter.

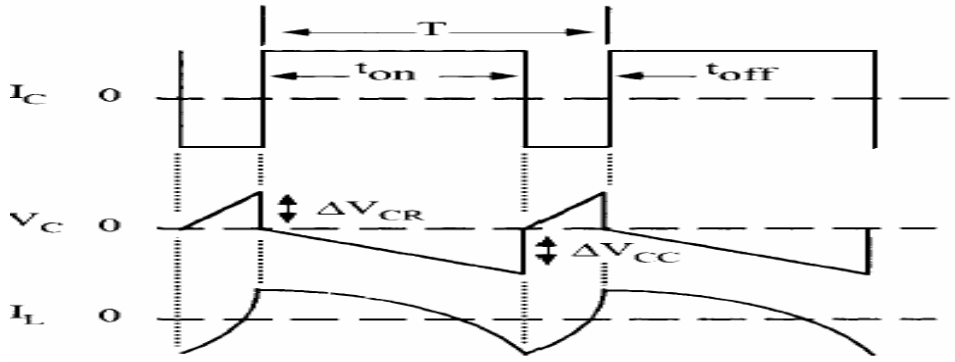

Figure 2.2 Typical Voltage, Current Waveforms

The filters traditionally used for attenuating ripple are passive low pass LC types. For high attenuation they must have low relatively frequencies (well below the switching frequency of the converter) and they can therefore interact dynamically with its control loop. The result can be ringing or even instability. Moreover, the low cutoff frequencies mean that the filter components must be large and heavy: despite the relatively small ripple signals, the series chokes must carry the full through current and the shunt capacitors must withstand the full applied voltage. Although LC filters are theoretically 100% efficient, in practice parasitic resistances, especially the winding resistances of chokes, reduce this benefit (Sheehan, 1979).

Switching regulators have required the engineer to put a significantly more analytical effort into the design of the input filter. The current pulse, induced by the switching regulator, has had the most impact on the input capacitor. These current pulses required the use of high quality capacitors with low equivalent series resistance (ESR). The waveforms, induced by the switching regulator, are shown in Figure 2.2. In the input inductor, L1, peak-peak ripple current is, I_L. In the capacitor, Cl peak-peak, ripple current is I_c. In the capacitor, Cl peak-peak, ripple voltage is, AVC. The equivalent circuit for the capacitor is shown in Figure 2.3. The voltage, ΔV_C, developed across the capacitor, is the sum of two components, the equivalent series resistance (ESR) and the reactance of the capacitor.

The voltage developed across the equivalent series resistance (ESR) is:

$$V_{CR} = I_C \left(ESR \right) \tag{2.1}$$

voltage developed across the capacitance is:

$$\Delta V_{CC} = I_C \left(\frac{\left(t_{on} \right)\left(t_{off} \right)}{\left(C1 \right)\left(T \right)} \right) \tag{2.2}$$

The sum of the two voltages, ΔV_{CR} and ΔV_{CC}, is:

$$\Delta V_C = \Delta V_{CR} + \Delta V_{CC} \tag{2.3}$$

2.1. Coupled Inductor Filter Modeling and Desing

When an inductance L is used to smooth a current i, the ripple voltage v appearing across it is non-zero. Since di/dt = v/L, the ripple current is also non-zero. But if L is coupled magnetically to a second choke, a voltage can be induced which, under the right conditions, cancels v. Because L sees a net voltage of zero, di/dt is zero, meaning that; has zero ripple. This technique is employed to good effect in the isolated Cuk converter (David, 1975) (Sheehan, 1979). Very low ripple is achieved at both input and output by coupling the input choke, the output choke and the transformer; with all the windings combined onto a single core, the size and weight of the converter is reduced.

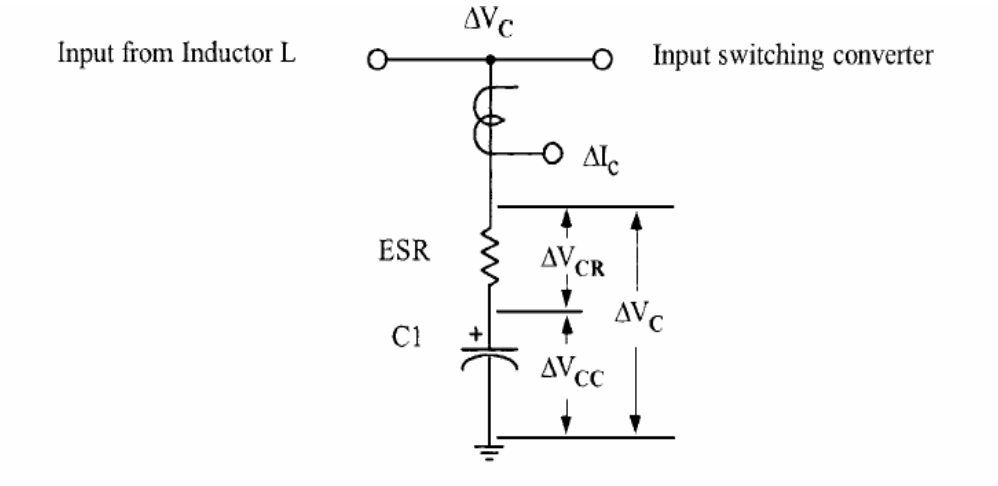

Figure 2.3 Capacitor, Individual Ripple, Components.

Like all nulling techniques, this one is not robust against parameter drift, and in practice a residual ripple current remains. Furthermore, large coupling capacitors are typically involved. As with conventional LC filters, the dynamics of the converter may be adversely affected and parasitic resistances cause losses

The input filter inductor is basically a straight-forward design. There are four parameters required to achieve a good design: (1) required inductance, (2) dc current, (3) dc resistance, and (4) temperature rise. The requirement for the input inductor is to provide a low ac ripple current to the source. The low ac ripple current in the

inductor produces an ac flux at a magnitude of about 0.025 tesla. This resulting low ac flux will keep the core loss to a minimum. The input inductor losses will normally be 80 to 90% copper. A high flux magnetic material is ideally suited in this application. Operating with a high dc flux and a low ac flux with its high flux density of 1.6 teslas, will produce the smallest size, as shown in Table 2.1.

Table 2.1 Most Commonly Used Input Filter Material.

Magnetic Material Properties		
Material	Operating Flux, B, tesla	Permeability Ui
Silicon Permalloy Powder Iron Power Ferrite	1.51.8 0.3 1.2-1.4 0.3	1.5K 14- 550 35-90 1K-15K

2.2. Filter Oscillation Problem

The input filter can affect the stability of the associated switching converter. The stability problem results from an interaction between the output impedance of the input filter and the input impedance of the switching converter. Oscillation occurs when the combined positive resistance of the LC filter, and power source exceed the negative dynamic resistance of the regulator's dc input. To prevent oscillation, the capacitor's ESR, and the inductor's resistance must provide sufficient damping. Oscillation will not occur when:

$$\left(\frac{\eta\left(V_{in}\right)^2}{P_o}\right) \rangle \left(\frac{L}{\frac{C+\left(R_L+R_S\right)\left(ESR\right)}{\left(R_L+R_S\right)+\left(ESR\right)}}\right) \qquad (2.4)$$

where η is the switching converter efficiency, $V_{in(max)}$ is the input voltage; P_o is the output power in watts, L is the input inductor in henrys; where, C, is the filter capacitor in farads, R_L is inductor series resistance in ohms; R_s is the source resistance in ohms, and R_d (ESR), is the equivalent series resistance in ohms. If additional damping is required, it can be done, by increasing the R_d (ESR), and/or RL

as shown in Figure 2.4. The series resistance, R_d, lowers the Q of the filter and kills the potential Oscillation.

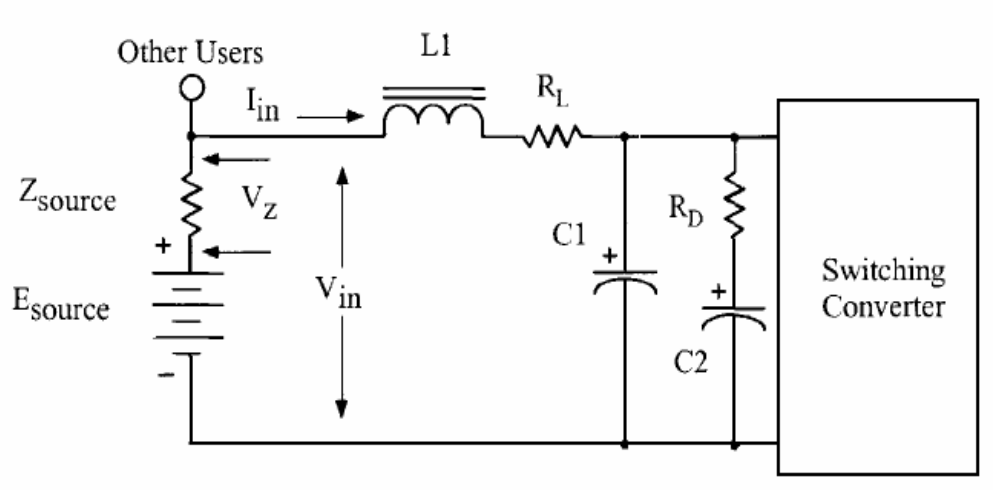

Figure 2.4 Input Filter, with Additional Damping

2.3. Filter Inrush Current Problem

The inrush current has always been a problem with this simple LC input filter. When a step input is applied, such as a relay or switch SI as shown in Figure 2.5, there is always a high inrush current.

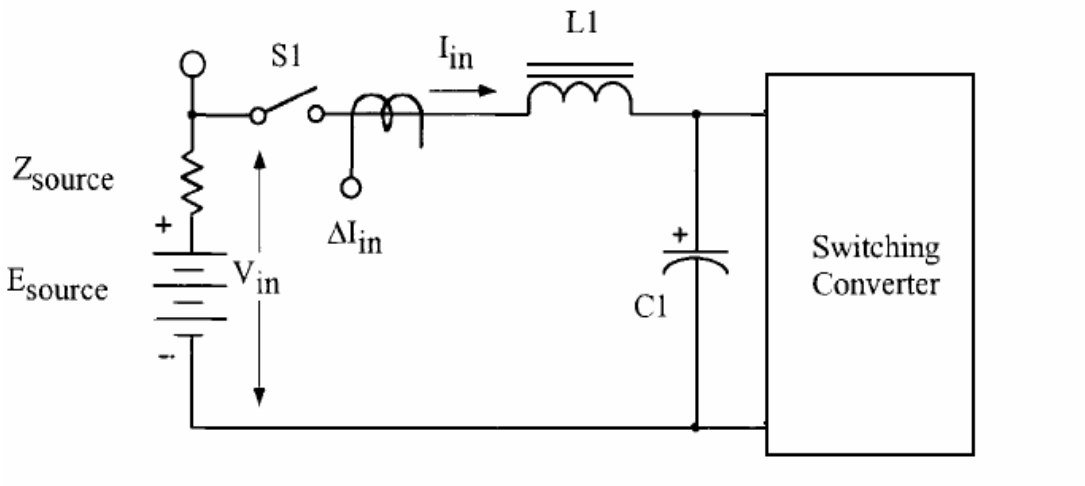

Figure 2.5 Input filter inrush current measurement.

When S1 is closed, the full input voltage, V_{in}, is applied directly across the input inductor, L1, because C1 is discharged. The applied input voltage, V_{in}, (volt-

seconds), to the input inductor, L1, and the dc current, (amp-turns), flowing through it is enough to saturate the core. The inductor, L1, is normally designed, using the upper limits of the flux density for minimum size. There are two types of core configurations commonly used for input inductor design: powder cores and gapped cores. Some engineers prefer to design around powder cores because they are simple and less hassle, while others design using gapped cores. It is strictly a game of trade-offs. Tests were performed using three different core materials: (1) powder core, (2) ferrite core, and (3) iron alloy. All three materials were designed to have the same inductance and the same dc resistance. The three-inductor designs were tested to compare the inrush current under the same conditions. The inrush current, AI, for all three materials is shown in Figure 2.6, using the test circuit, shown in Figure 2.5 (Phelps & Tale, 1979).

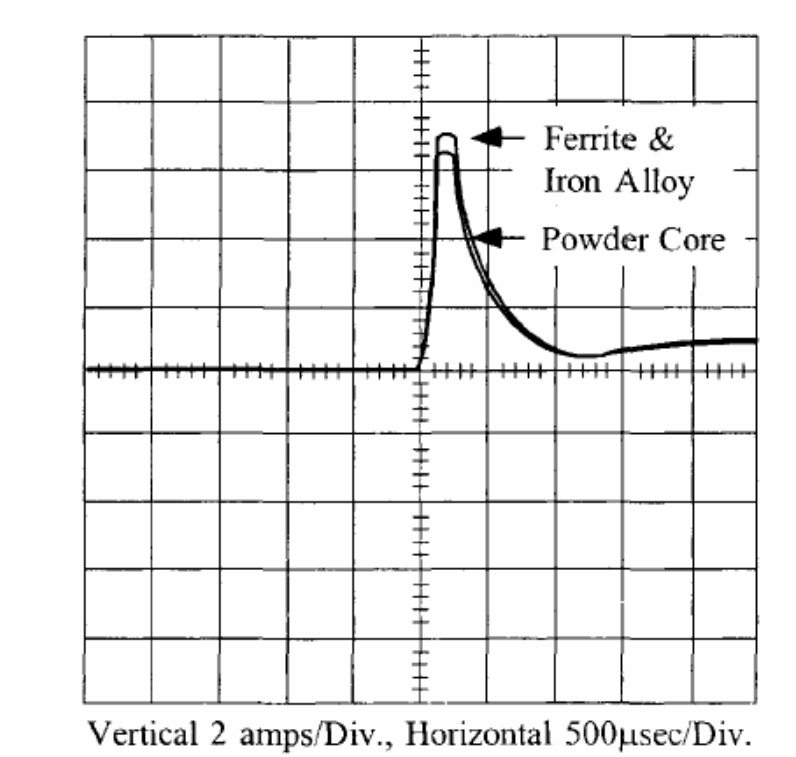

Figure 2.6 Typical, inrush current for a simple input.

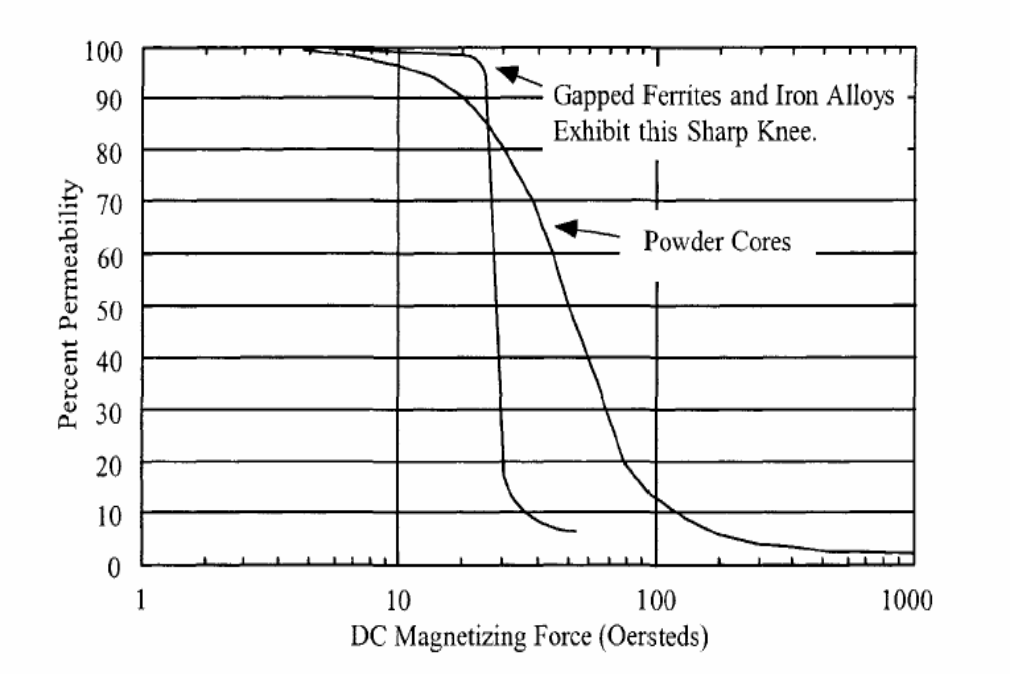

Figure 2.7 Comparing gapped and powder cores, permeability change with DC bias.

2.4. Resonant Charge

Most all types of electronic equipment are energized by either a switch or relay. This type of turn-on goes for aircraft, computer, medical equipment, and automobiles. There are some power sources that require some type of current limiting that does not follow the general rule. If the input voltage is applied via a switch or relay to an input filter, as shown in Figure 2.8, a resonant charge condition will develop with L1 and C1. The resulting resonant charge with L1 and C1 could put a potential on C1 that could be as much as twice the applied input voltage, as shown in Figure 2.9. The voltage rating of C1 must be high enough to sustain this peak voltage without damage. The oscillating voltage is applied to the switching converter.

A simple way to dampen this oscillation is to place one or two diodes across the input choke, as shown in Figure 2.10. The reason for two diodes is the ripple voltage, V_c, might be greater than the threshold voltage of the diode. As the voltage across C1 rises above the input voltage, V_{in}, due to the oscillation, diodes CR1 and CR2 will

become forward-biased, clamping the voltage across C1 to two diode drops above the input voltage, V_{in}, as shown in Figure 2.11.

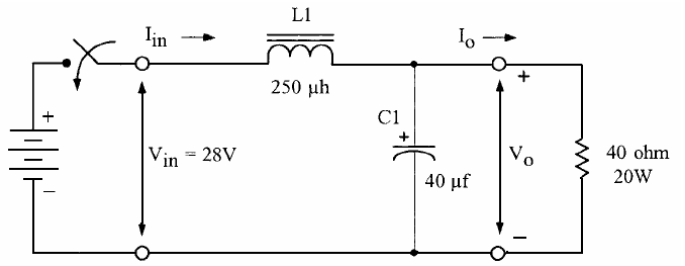

Figure 2.8 Typical LC input filter.

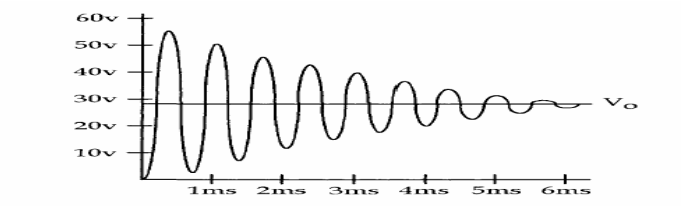

Figure 2.9 Resonating voltage, across capacitor, C1.

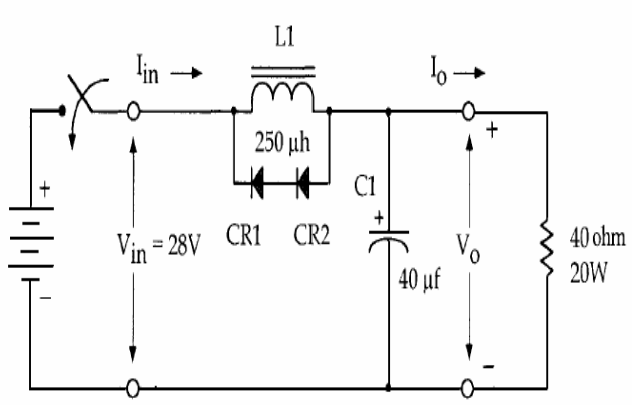

Figure 2.10 Input inductor with clamp diodes

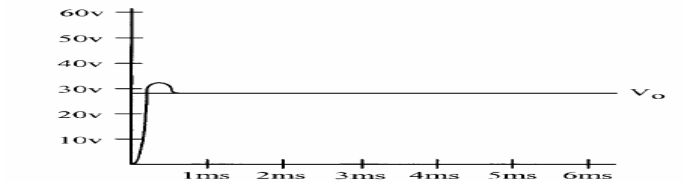

Figure 2.11 DC Voltage across C1, with the clamp diodes, note that oscillations stopped by this way

2.5. Input Filter Inductor Design Procedure

The input filter inductor LI for this design is shown in Figure 2.12.

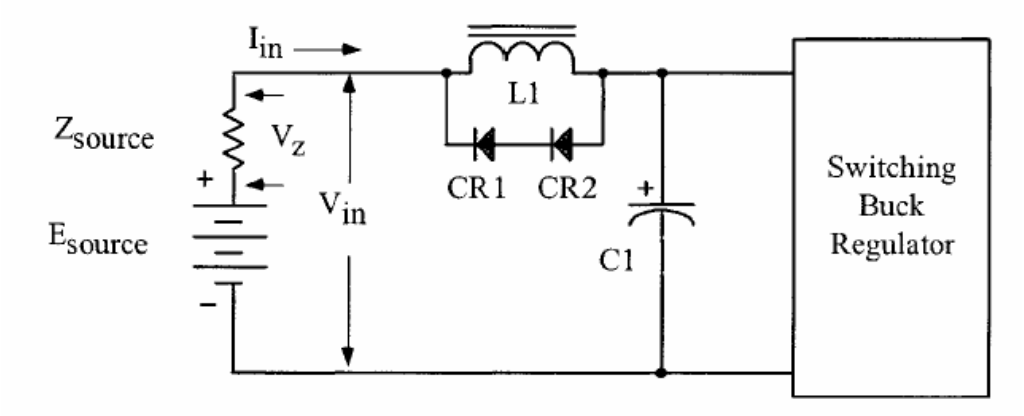

Figure 2.12 Input filter circuit.

The ac voltages and currents associated with the input capacitor, C1, are shown in Figure 2.13.

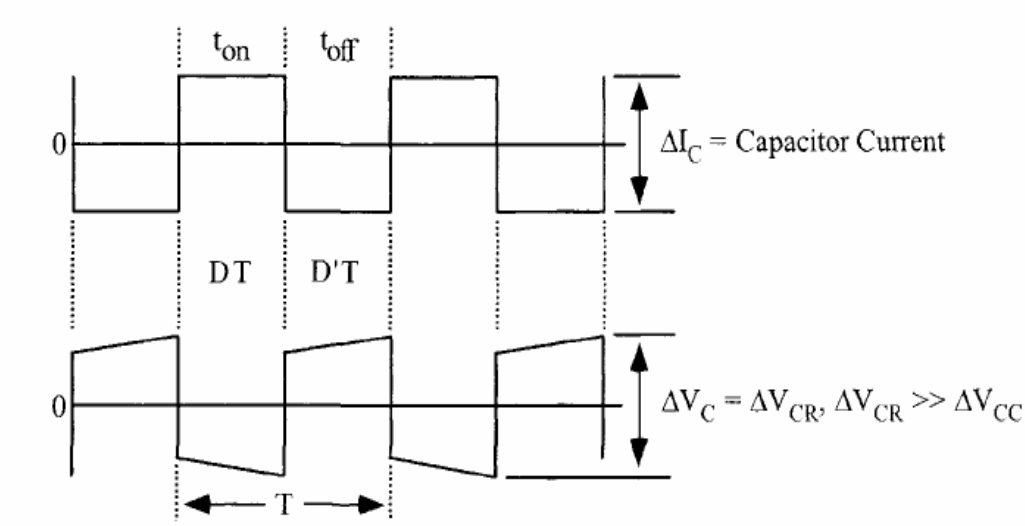

Figure 2.13 Input capacitor voltage and current ripple.

The components of the inductor current, due to, AV_{CR} and AV_{CC}, are:

ΔV_{CR} = Peak to Peak component due to capacitor, ESR.

Δ Vcc = Peak to Peak component due to capacitor.

M_{LR} = Component of the inductor ripple current developed by $\&V_{CR}$.

AI_{LC} = Component of the inductor ripple current developed by A V_{cc}.

$$\Delta I_{LR} = \left(\frac{\Delta V_{CR}}{L}\right)\left(DD'T\right)$$
$$\Delta I_{LC} = \left(\frac{\Delta V_{CC}}{2L}\right)\left(\frac{T}{4}\right) \tag{2.5}$$

It will be considered that, AI_{LR}, dominates because of the capacitor, ESR, so:

$$\Delta I_{LR} = \left(\frac{\Delta V_{CR}}{L}\right)\left(DD'T\right) \tag{2.6}$$

The ac voltages and currents impressed on the input capacitor, C1, are defined in Figure 2.3.

CHAPTER THREE
ACTIVE FILTER DESIGN

The drive to higher switching frequencies in power circuits is motivated by the smaller energy storage elements that supposedly result. As the switching frequency of a power circuit is pushed toward 1 MHz, however, the allowable input-output ripple levels are often much more strict than they were at lower frequencies and much of the desired filter size reduction cannot be achieved.

For example, in the vicinity of 1 MHz, MIL-STD-461B CE03, a military current ripple specification shown in Fig. 3.1, is decreasing at 30 dB/decade. Thus, a second-order passive LC filter designed to meet this specification at 100 kHz exceeds it by only 10 dB at 1 MHz. This corresponds to a filter energy storage reduction of only 1.8 instead of the 10 that was sought. So, switching power converters inherently generate ripple, and typically require input and output filtration to meet ripple and EMI specifications (Casey, Goldberg & Schlecht, 1988).

Figure 3.1 MIL-STD-461B CEO3 current ripple specification.

Furthermore, the ripple limitations of several military and commercial specifications in this frequency range call for maximum input and output ripple levels on the order of 20 μA and 200 μV, regardless of the power level of the

converter. Medium and large power circuits, switching several amps and volts, therefore need very large ripple attenuation at both their input and output. For such high attenuations, second-order *LC* filters are generally not practical, and third- or fourth-order filters must be employed. Though they result in significantly smaller filter elements, these higher order filters can make compensation of a closed-loop control very difficult. Passive LC low-pass filters have traditionally been employed to achieve the necessary degree of ripple attenuation (Silber, 1975). The passive filter components often account for a large portion of converter size, weight, and cost (Silber, 1975) ,(Zhu, Perreaul, Çalışkan and other). Furthermore the temperature and reliability limitations of filter capacitors can present a significant design constraint.

Fortunately, a salient feature of all the passive LC filters is that, while all the elements have to be sized to handle the full quiescent energies present, most of the elements see only very small ripple energies. Active circuits, constructed to see only the ripple energies, can therefore replace these elements. Although the overall filter is more complicated and the ripple energies are then dissipated, these losses are easily offset by the savings in size, weight, and cost of the large passive elements in the original filter.

In general, active ripple filters are linear amplifier circuits that exchange the performance of passive impedances. The active filter may either increase the effective impedance of series path or reduce the effective impedance of shunt path. For example, as illustrated in Fig 3.2 (a) a series active filter introduces a voltage in series with a noise source, effectively increasing the impedance of that series path to noise currents. Similarly, a shunt active ripple filter is placed in shunt with a noise source, reducing the effective impedance of shunt path as shown in Fig 3.2 (b). A variety of filter structures and control methods are possible, but generally conform to one or both of these approaches.

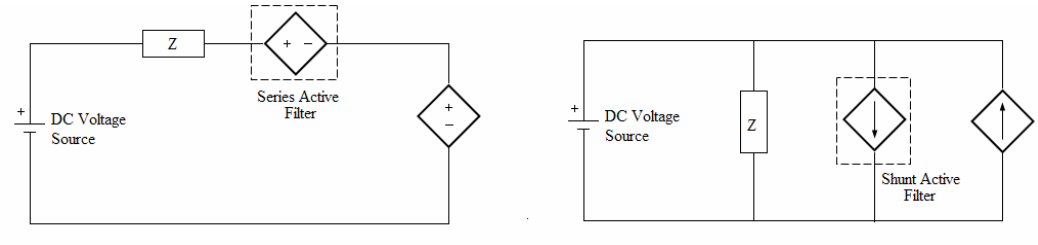

Figure 3.2. (a) Series active filter topology, (b) Shunt active filter topology.

Active filters may be characterized by whether they inject ripple voltages (Feng, Sander & 1970) (LaWhite & Schlech, bt) or currents (Zhu and other, 1999) (Hamill, 1996) (Midya & Krein bt.) in the circuit to achieve ripple reduction. Controls governing the ripple correction can be derived through either feedforward (Zhu and other, 1999) (Moon & Cho, 1996) (Midya & Krein bt.) or feedback (Poon, Liu, Tse & Pong, bt). (Farkas & Schlect, 1994) Feedforward filters sense a ripple component and inject its inverse, while feedback filters suppress ripple via high-gain feedback control. Combinations of these mechanisms are also possible (Feng, Sender & Wilson, 1970), and there are a wide variety of means for implementing the sensing and injection functions.

Noise suppression control can be achieved through feedforward and/or feedback. Feedforward control relies on a small bar precise gain. For a perfect feedforward path gain of unity, the ripple would be entirely cancelled. However, due to gain and phase accuracy limitations in the components, feedforward cancellation alone cannot fully attenuate the ripple. On the other hand, feedback relies on a large but possibly imprecise gain. The feedback gain is directly proportional to the ripple suppression. In other words, the larger the gain the grater the ripple attenuation; an infinite gain would yield zero ripple. Stability considerations limit the achievable feedback suppression. A combination of both feedback and feedforward control is also possible.

3.1. Topologies of Active Filters

Ripple filters may equally well be applied to the output of a converter or to its input, the case considered here. The application of interest was obtaining low input

ripple current for converters drawing about 40 W from the dc bus of a spacecraft. The configuration is shown in Fig. 3.3. For various reasons (Sullivan, 1989) it is often desirable to distribute the power around a spacecraft at a regulated voltage of about 30-50 V, transforming it to the required end voltage by dc-dc conversion in each payload module. If standardized converters are employed, their switching frequencies will be similar. There is a risk that the ripple currents might drift into phase; worse, the converters, interacting via the bus impedance, might even lock together. The total ripple current drawn from the bus would then be large, and might interfere with other equipment, in extreme cases causing malfunctions.

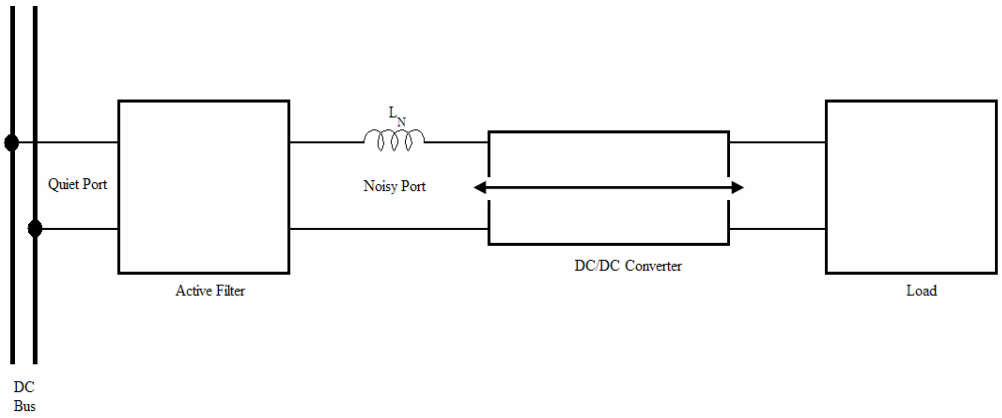

Figure 3.3 Active filter employed to smooth current drawn from spacecraft dc bus.

Because ripple current is of interest here, a current canceling filter was chosen. The basic topology comprises the two-port T network shown in Figs. 3.5 and 3.6. Considering the dc equivalent circuit (Fig. 3.5), one port acts as the input, being connected to the dc source, while the other acts as the output. For ac ripple (Fig. 3.6), one port is noisy, being connected to the switching converter, while the other is quiet (nominally ripple free). Note that the association between input/output and quiet/noisy depends on the application. When, as in Fig. 3.4, the filter is placed in the feed to a dc-dc converter, the input is quiet and the output is noisy. On the other hand, when the filter is placed between a converter and its load, the input is noisy and the output is quiet.

The topology employs two current sensors for improved performance: one for feedforward, the other for feedback. The feedforward works by sensing the ripple

current at the noisy port and generating an identical current (ideally) in the vertical leg of the T, leaving zero ripple current at the quiet port. For perfect ripple cancellation the current gain Bp would have to be exactly unity, at all frequencies and amplitudes of interest. This is impossible given the limited bandwidth and nonlinearities of the components involved. Moreover, being a nulling method, feedforward is sensitive to component value drift. Matters could be improved by means of an adaptive null seeking arrangement (Midya & Krein, bt).

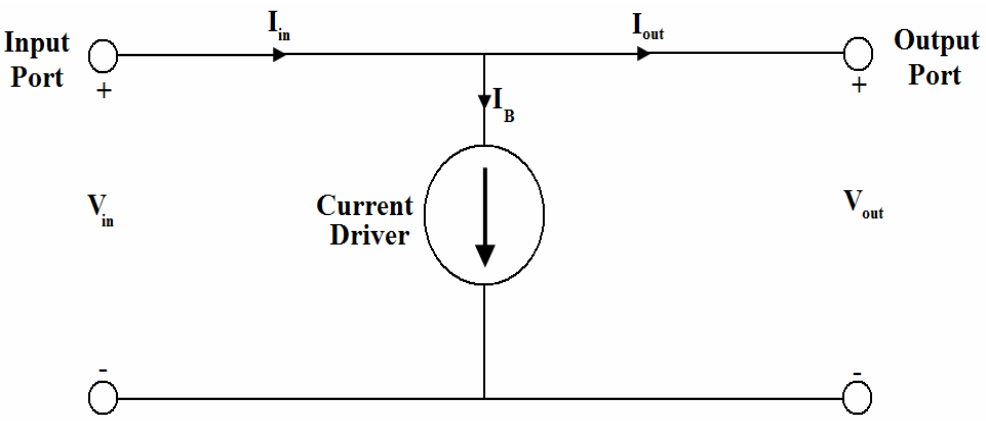

Figure 3.4. DC equivalent circuit of active filter.

The feedback works by sensing the ripple current at the quiet port and driving it towards the desired value of zero. Because this is an error driven system, infinite loop gain would be needed for perfect ripple cancellation. In practice, to avoid instability the loop gain must be restricted at high frequencies, resulting in limited ripple attenuation.

Good overall performance can be achieved by a combination of feedforward and feedback, but at the price of an additional current sensor and a little extra circuitry.

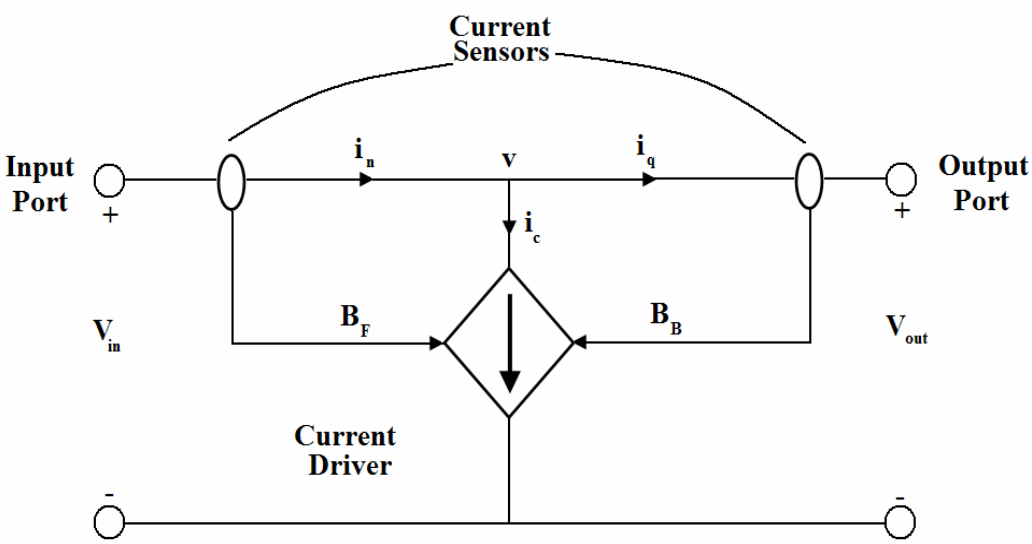

Figure 3.5. AC equivalent of active filter, showing feedforward and feedback paths.

It is presently seen that active filters for power circuits can be divided into four distinct topologies, as depicted in Fig. 3.5. In these circuits, Vex, or Zext model either the dc power source or the load for the converter, while I, or V, model the square wave action of the switches within the converter.

3.2. Analysis

3.2.1. Ripple Attenuation With Active Filters

In an ideal filter, the ripple current iq at the quiet port would be zero. (Fig. 3.5 for symbols.) Thus the whole of the unwanted ripple current i_n at the noisy port would be diverted down the vertical leg of the T and back to the noisy port. To this end a cancellation current $i_c = i_n$ should be generated in the vertical leg. From Fig. 3.6, the cancellation current is given by (Hamill, 1996)

$$I_c = B_F I_n + B_B I_q \tag{3.1}$$

where B_F and B_B are the current gains of the feedforward and feedback paths, respectively, and I_c is the Laplace transform of $i_c(t)$, etc. (All quantities in (3.1) are functions of the complex frequency s.) In reality I_c does not match I_n exactly, so the

quiet port current $I_q = I_n - I_c$ is non-zero. The closed-loop current transfer function B can be found as

$$B = \frac{I_q}{I_n} = \frac{1 - B_F}{1 + B_B} \tag{3.2}$$

For good ripple attenuation the current gain B should be small as possible, so B_F is ideally unity, while B_B is ideally infinite.

3.2.2. Stability

When considered in isolation, the stability of the active filter is determined by the poles of the transfer function B(s): they must lie in the left half of the complex plane.

When embedded within a system, the active filter will interact with its neighboring circuitry, and its stability then depends on the external impedances. Fig. 3.5 shows the noisy port fed by a Thevenin equivalent source of voltage V_n in series with impedance Z_n, while the quiet port sees V_q in series with Z_q. The voltage V appearing across the vertical leg of the T can be found as

$$V = \frac{V_n}{1 + \dfrac{Z_n}{Z_q B}} + \frac{V_q}{1 + \dfrac{Z_q B}{Z_n}} \tag{3.3}$$

where B is given by (3.2). The values of Z_n and Z_q include the impedances of the respective current sensors and interconnect. (In certain cases, Z_n may even have a negative resistive component, e.g., when the noisy port is connected to the input of a converter with a constant power characteristic.) For system stability, the poles of $V(s)/V_n(s)$ and $V(s)/V_q(s)$ must all lie in the left half plane.

It is reassuring that, in the limit as $B \to 0$, the term $Z_qB/Z_n \to 0$, so $V \to Vq$ and the system is stable. Since B = 0 would be achieved with the ideal feedforward

current gain of unity, it is arguable that one effect of the feedforward is to enhance the system stability.

In the practical case where |B| > 0, system stability can be improved by modifying the impedances. Since $Z_qB/Zn \rightarrow 0$ if $|Z_n| >> |Z_q|$, it helps to make $|Z_n|$ large (e.g., by inserting inductance L_n in series with the noisy port, as in Fig. 3.4), and for $|Z_q|$ to be small (a characteristic of a well designed dc bus).

3.2.3. Response to Bus Ripple

A question that arises in this application is the response of the active filter to ripple voltages on the dc bus. Will it attempt to smooth the bus voltage by trying to absorb all the ripple current injected by other equipment connected to the bus. Analysis of Fig. 3.6 yields.

$$\begin{aligned} I_n &= \left(V_n - V_q\right)\Big/\left(Z_n + BZ_q\right) \\ I_q &= \left(V_n - V_q\right)\Big/\left(Z_n/B + Z_q\right) \\ I_c &= \left(1-B\right)\left(V_n - V_q\right)\Big/\left(Z_n + BZ_q\right) \end{aligned} \qquad (3.4)$$

where B is given by (3.2). Since the system is linear, superposition applies and V_n may be set to zero without loss of generality. Consider the following two extreme cases.

1. *Active filter not present.* This is emulated by setting *B=1*, making $I_n = I_q = -V_q\Big/\left(Z_n + Z_q\right)$ and $I_c = 0$. Thus a ripple current of $-V_q/(Z_n + Z_q)$ flows from the bus through the input of the converter.

2. *Ideal active filter present*. In this case *B=0* making $I_q = 0$: no ripple current is drawn from the bus. However, $I_c = -V_q\big/Z_n$, i.e., a ripple current of $-V_q/Z_n$ circulates through the current driver and the input of the converter.

The practical case will be close to the latter. If $|Z_n| >> |Z_q|$, as desirable for stability, then there will be a slight increase in the current circulating through the input of the converter when the active filter is inserted. Instead of flowing from the bus, it flows through the current driver, which must be properly sized to carry it.

To summarize, the active filter does not try to sink a large ripple current from the bus. On the contrary, it drives this current towards zero. However, the current circulating through the input of the converter due to bus voltage ripple is almost the same as without the active filter.

3.2.4. Efficiency

In the ideal dc circuit of Fig. 3.4, $V_I = V_O$. For perfect efficiency, $I_I = I_O$. In practice the vertical leg may need to pass a bias current I_B, depending on the type of current driver employed. The efficiency is then $\eta = I_O / I_I$

In the design, the current driver may for example consist of a pair of metal-oxide-semiconductor field-effect transistors (MOSFETs) biased to work in Class A. Their drain currents comprise the bias dc I_B with the ripple cancellation current i_c superimposed. To avoid distortion, the total current must never go to zero: $I_B + i_c(t) > 0$ for all t . Now for ideal cancellation $i_c = i_n$, so $I_B \geq I_{n(-pk)}$, where $I_{n(-pk)}$ is the negative peak value of in (t); thus the bias current can be chosen. Suppose the limiting case of $I_B = I_{n(-pk)}$ taken. Since $I_I = I_O + I_B$, and defining a peak ripple factor $r = I_{n(-pk)} / I_O$, the efficiency is

$$\eta = \frac{1}{1+r} \tag{3.5}$$

(This expression neglects control circuit and other losses.) The efficiency drops as r increases, suggesting that the active filter is inappropriate for high ripple factors. However, if $r < 0.05$, which should b e easily achieved with a little passive filtering, the efficiency will exceed 95%, adequate for most purposes.

3.3. Active Ripple Filter Design for DC/DC Converters

Active filters offer an alternative approach. In low frequency applications, e.g. at 50-60 Hz, switched-mode techniques can be employed. But to cope with the frequencies emitted from dc-dc converters, which range from tens of kilohertz to megahertz, nonswitched "linear" circuits must be used (Walker, 1984). Their inherent dissipation makes them less than ideal, but the overall efficiency can nevertheless be acceptable.

Active ripple filter topologies are of two basic types, which are duals. In voltage canceling filters, a voltage is introduced in series with the ripple voltage to cancel it. (This is reminiscent of the coupled inductor technique.) In current canceling filters, a cancellation current is injected at a node traversed by the ripple current. An alternative classification, due to LaWhite and Schlecht (Farkas & Schlecht 1994) (White & Schlecht 1987) (White & Schlect (1988) is in terms of the ripple quantity sensed (current or voltage) and the means of applying the cancellation signal (by a current or voltage source). Active ripple filters arc then classified as voltage or current sensing, voltage or current driving.

In all the DC/DC converters, output voltage has a high frequency ripple. Frequency of this ripple voltage is a multiple of switching frequency. In modern DC/DC converters, to decrease the size and cost of inductors and capacitors, higher switching frequencies are utilized. Typically, the frequency of the voltage ripple is more than 150 KHz, which is in the range of EMI noises for automotive systems. Load at the output of DC/DC converter draws a current with the same or higher ripple frequency. This ripple is larger in high current and low output voltage converters such as the ones used in automotive systems. Additionally, output capacitor has an Equivalent Series Resistance (ESR) that contributes to the ripple voltage. Ceramic capacitors have lower ESR but are expensive for higher capacitance values. Aluminum electrolytic and tantalum capacitors are relatively inexpensive for higher capacitance values but their ESR is much higher (Nasiri, 2005).

Figure 3.6 shows a flyback DC/DC converter and its output voltage ripple. The ripple of output voltage for this converter is as following:

$$\Delta V_0 = \frac{I_L D}{f_s C_{DC}} \tag{3.6}$$

where f_S is the switching frequency of the converter, ΔV_O is the ripple voltage, and D is the duty ratio of Q_1.

Traditionally, LC passive filters have been used to compensate this ripple. For proper mitigation, this passive filter must have wide frequency band. Additionally, the performance of low order passive filters is not satisfactory and higher order passive filters are needed. These characteristics increase size and, consequently, weight and cost of the passive filters. Performance and controllability of the closed loop system also decreases in the presence of high order passive filters. On the other hand, change of the parameters of the passive filters with time and environmental conditions decrease the attenuation of the passive filters. These problems justify using the active ripple filters.

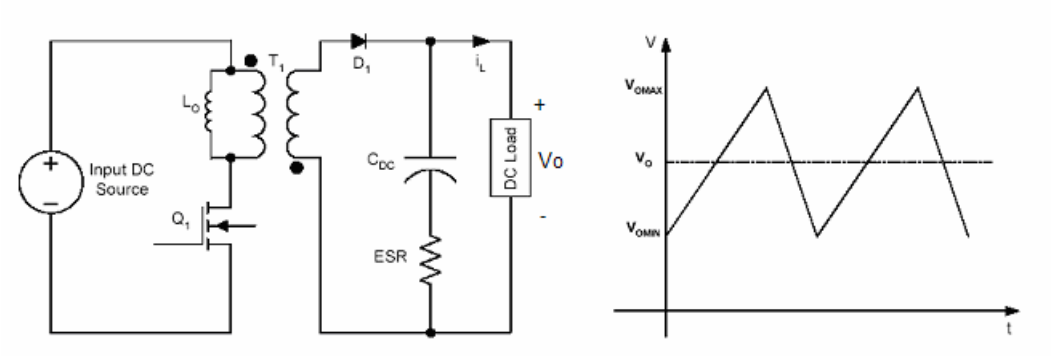

(a)

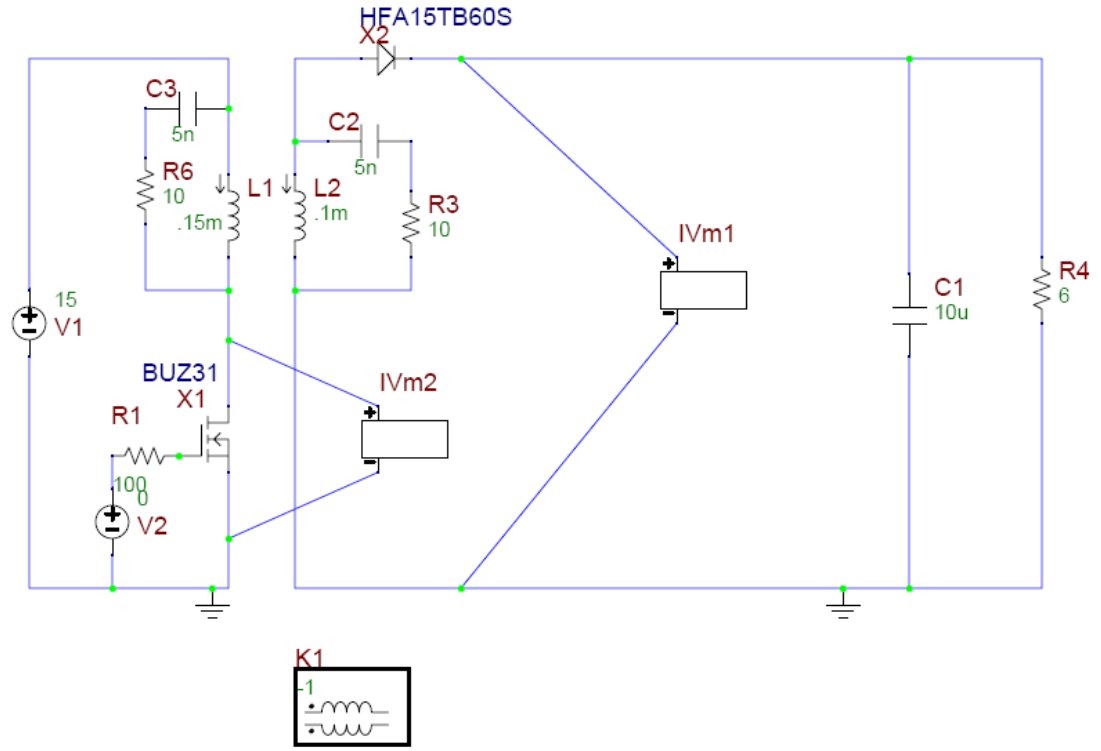

(b)

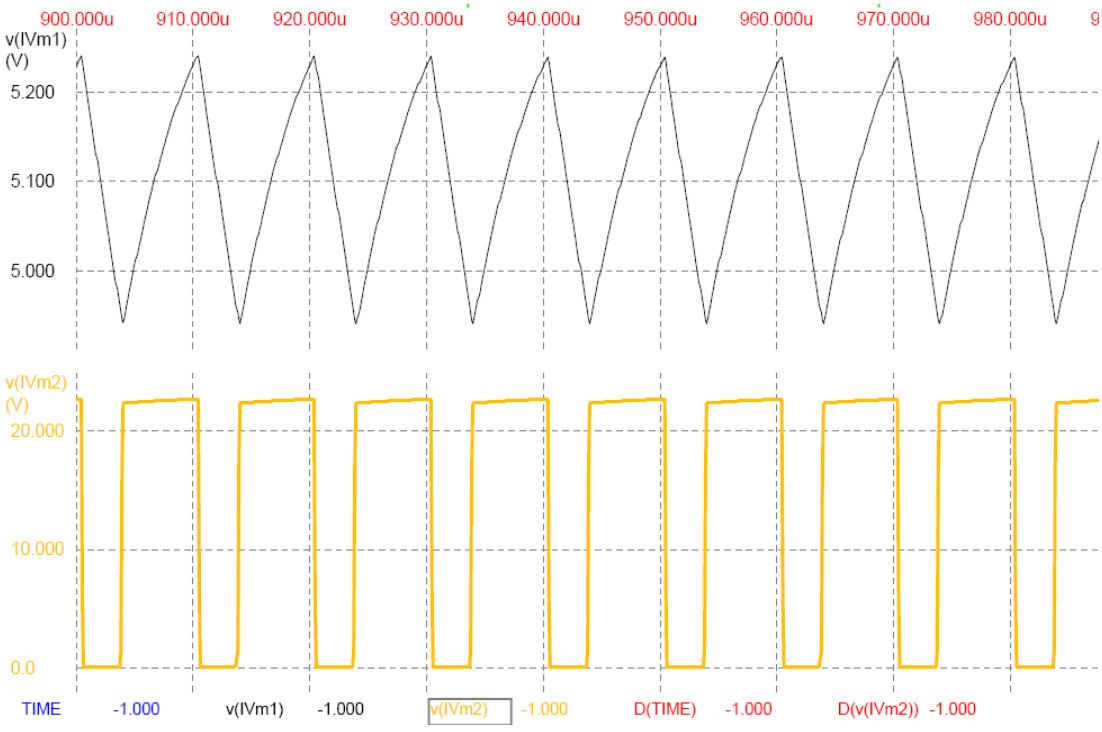

(c)

Figure 3.6. (a) Configuration of a Flyback DC/DC converter and its output voltage ripple.(b) Pspice simulation model.(c) Result of the circuit figure 3.6.b

Active ripple filters with robust characteristics and better attenuation can provide an alternative for passive filters (Farkas & Schlect, 1994) (Midya & Krein, 1994) (Zhu and other 2005). There is an energy difference between passive and active filtering. Passive filters absorb the energy of ripples and trade it with the system but active filters dissipate the energy of the ripples. Another passive method for decreasing current ripple in DC/DC converters is using coupled inductors. By using coupled inductors, the voltage over output inductor of the converter can be forced to zero and, consequently, ripple of current will be zero. Great saving in size, weight, and cost can be achieved from this method. Unfortunately, this method is not applicable to all type of DC/DC converters. Additionally, changes of converter parameters with time and temperature do not allow proper cancellation of the ripple current.

Four possible configurations for active ripple filters are shown in Figure 3.7. Two configurations are current-based and two others are voltage-based. Figure 3.7 (a) shows a current ripple active filter with current feedbacks. For better performance, active filter is composed of both feed forward and feed back controllers. In figure 3.7 (a), we have:

$$i_s + i_f = i_r \tag{3.7}$$

where i_s is the ripple current of the sending end and ir is the ripple current of the receiving end. if is the current of the active filter. Since the active filter is composed of two feed forward and feed back controllers, we have:

$$i_f = Ki_s + Ai_r \tag{3.8}$$

where K is the gain of the feed forward amplifier and A is the gain of the feed back amplifier. With substituting (3.7) in (3.8), we have:

$$i_r = \frac{i_s(1+K)}{(1-A)} \tag{3.9}$$

Since we want to have i_r =0, for ripple frequency K must have a magnitude of one with a phase of 180 degrees. Feed back amplifier must have high gain. Ideally, feed forward amplifier injects a current, which is the same as the current ripple in the reverse direction and therefore, the output ripple will be set to zero. However, because of the non-ideality and constraints on sensors and amplifiers, feed back controller is used to mitigate the residual ripple.

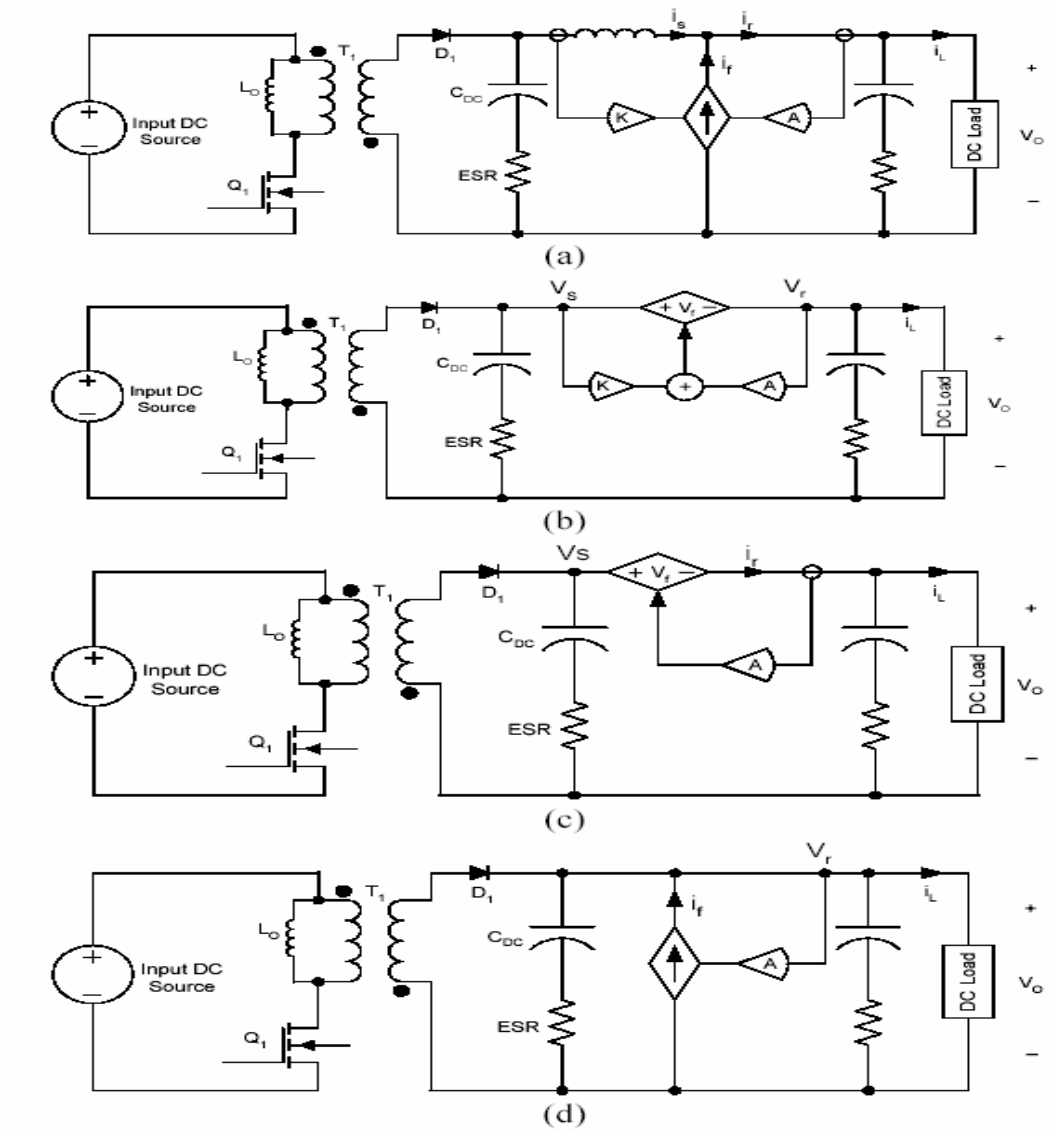

Figure 3.7. Four possible topologies for active ripple filters

Figure 3.7 (b) shows a voltage-based active ripple filter. Similar to the current active filter, both feed forward and feed back controllers are used. This configuration

is dual of the circuit shown in Figure 3.7 (a). We have the same equation for this configuration:

$$V_s + V_f = V_r \tag{3.10}$$

$$V_f = KV_s + AV_r \tag{3.11}$$

$$V_r = \frac{V_s(1+K)}{1-A} \tag{3.12}$$

where V_r is the ripple voltage of the receiving end and V_s is the ripple voltage of the sending end. K and A should have the same characteristics as mentioned above for parameters of figure 3.7 (a).

Figure 3.7 (c) shows a voltage active filter with current feedback. In this configuration, for ripple frequency, voltage active filter works as a large series resistor to limit the ripple current but it shows zero resistance at lower frequencies. The equivalent circuit of this configuration is shown in Figure 3.8 (a). The system equations are as following:

$$V_f = Ai_r \tag{3.13}$$

$$V_{0r} = \frac{Z_0}{Z_0 + A_r} V_{sr} \tag{3.14}$$

$$Z_0 = \frac{R_0 + 2\pi L_0 f_r + 2\pi(ESR)R_0 C_{DC} f_r + 4\pi^2 (ESR)L_0 C_{DC} f_r^{\,2}}{1 + 2\pi(R_0 + ESR) + 4\pi^2 L_0 C_{DC} f_r^{\,2}} \tag{3.15}$$

The simulation result for this topology is shown in Figure 3.8 (b) when the gain of the current feedback is set on 10. Output voltage ripple of Figure 3.6 (b) is applied to the system (Nasiri, 2005).

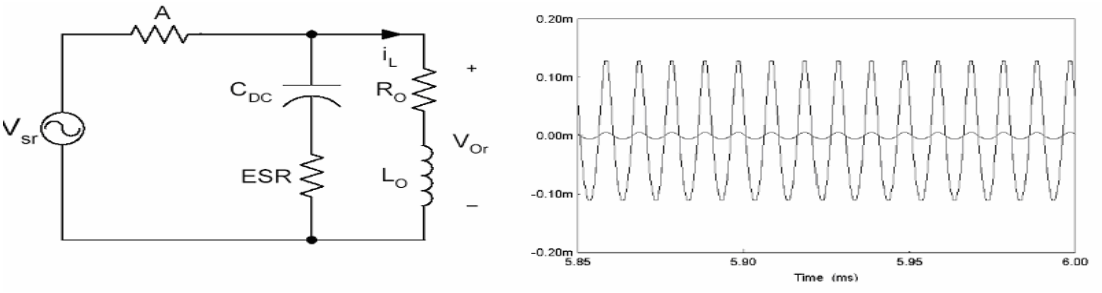

(a)

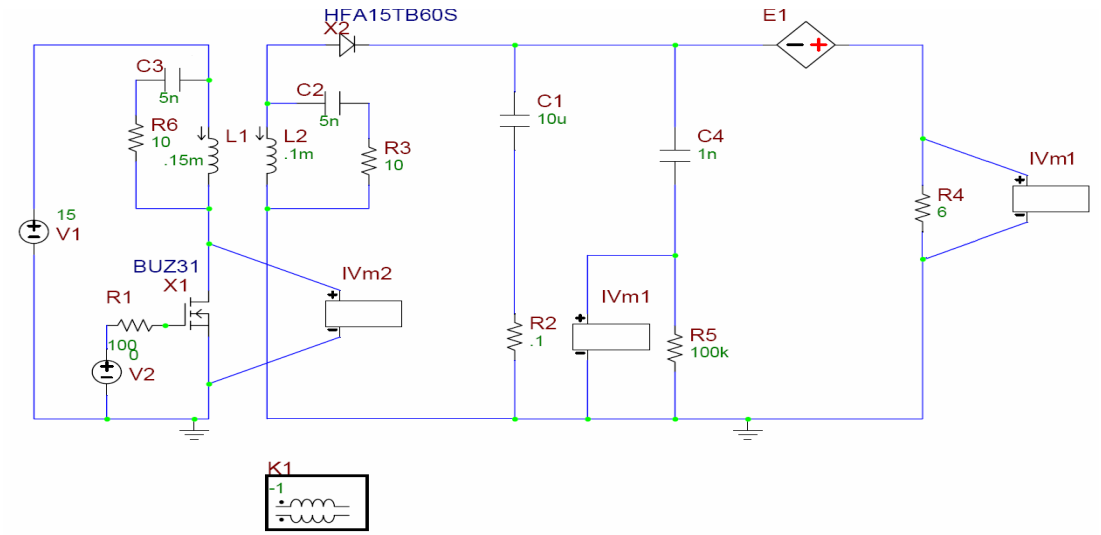

(b)

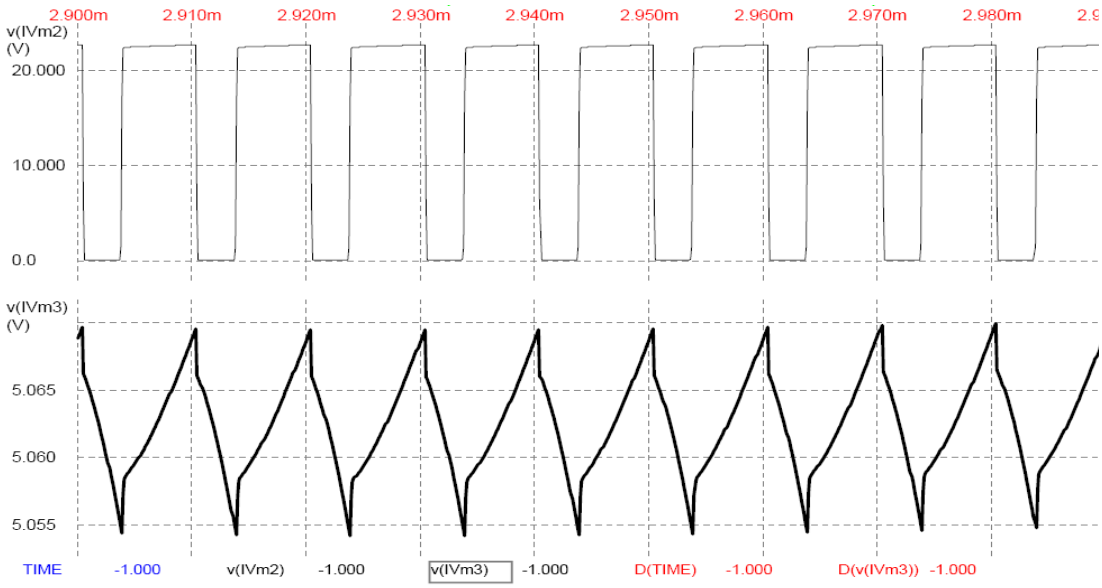

Figure 3.8. (a)The ripple equivalent circuit of configuration shown in Figure 3.7 (c) and the output ripple without active filter. (b) Pspice simulation model of Figure 3.7.c (c) Result of the circuit in figure 3.8.b

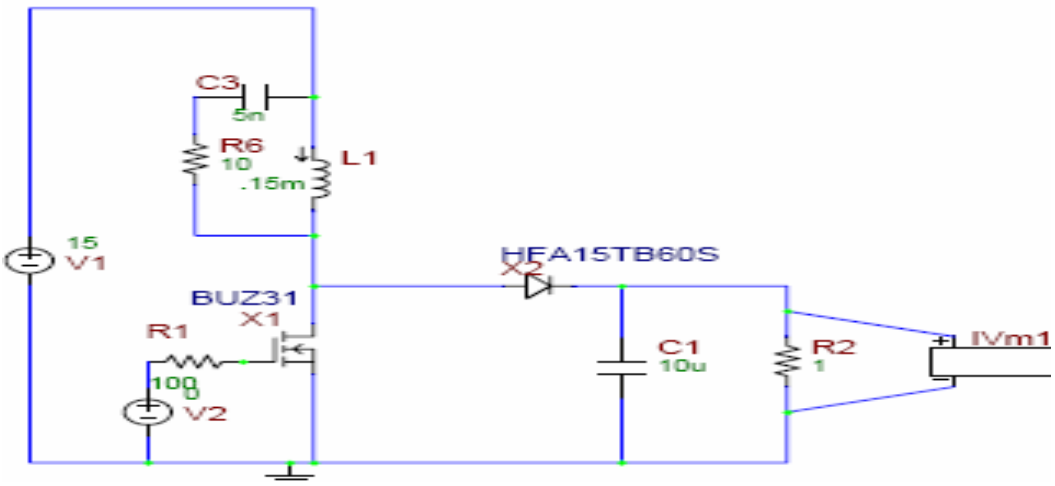

(a)

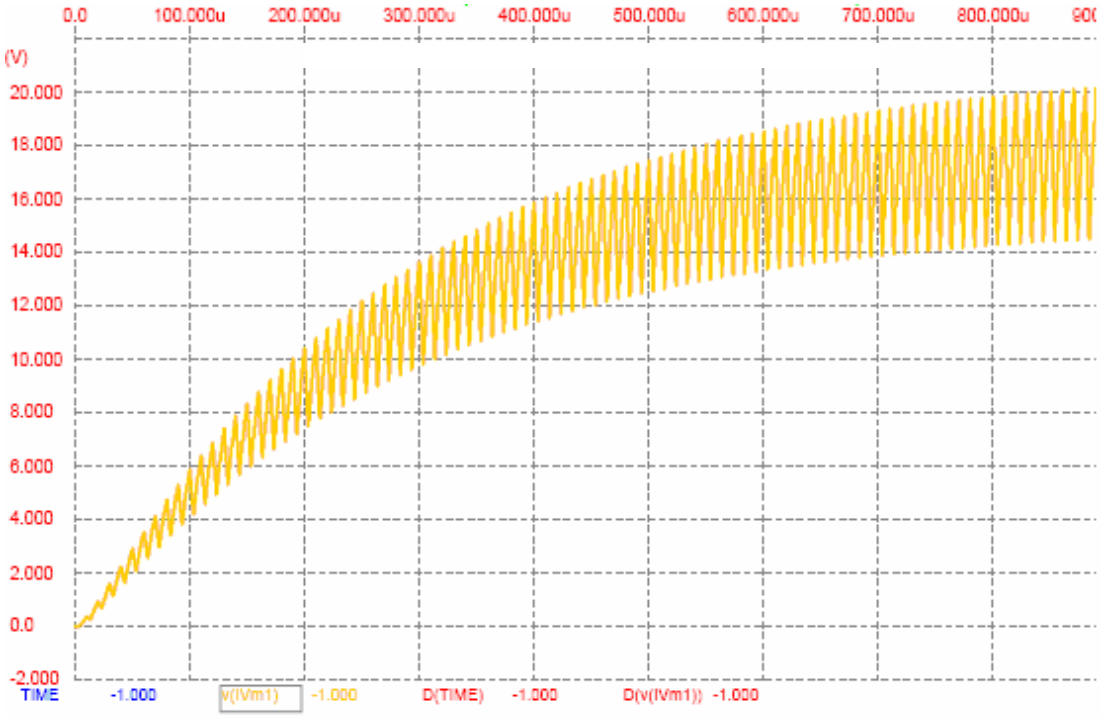

(b)

Figure 3.9. (a) It is the circuit whitout active filter (b) Result of the circuit in figure 3.9.a

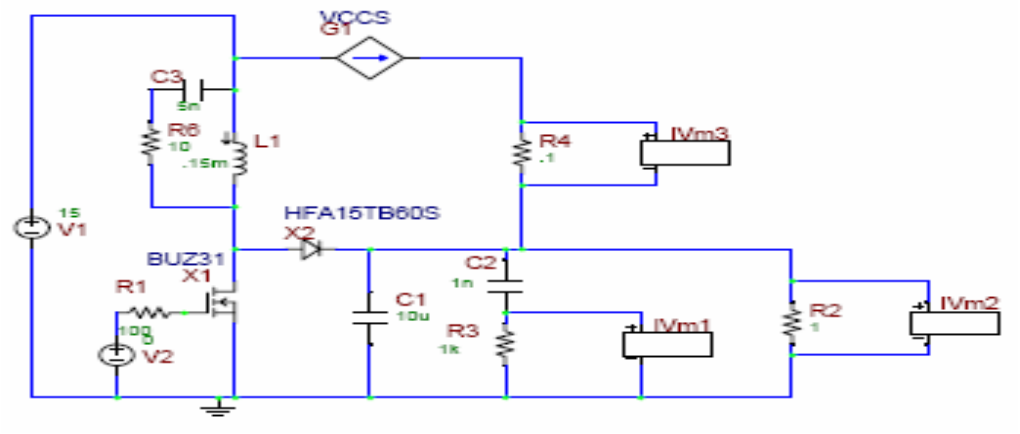

(a)

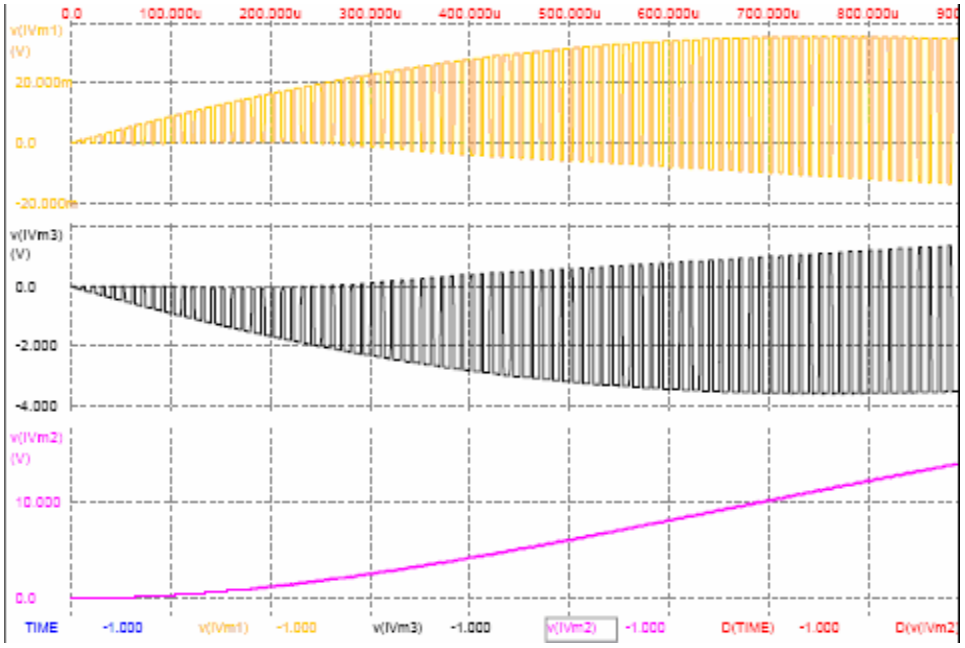

(b)

Figure 3.10. (a) It is the circuit whith active filter (b) Result of the circuit in figure 3.10.a

Figure 3.7 (d) shows the configuration of current active filter with voltage feedback. The system equations are as following:

$$i_r = \frac{V_r}{Z_o} \tag{3.16}$$

$$i_f = AV_r \tag{3.17}$$

To cancel the output ripple voltage we must have:

$$i_f = -i_r \tag{3.18}$$

Therefore:

$$A = -\frac{1}{Z_0} \tag{3.19}$$

Equation (3.19) means that the feedback gain must be equal with admittance seen at the output stage of the converter. This feature makes the controlling of this topology very cumbersome because the output admittance is variable and load dependent.

3.3.1. Current Sensors

Different kinds of high frequency current sensors can be used for ripple current sensing on the configurations shown in Figure 3.7. Optimum current sensors must have high sensitivity, wide frequency range, and zero phase shift.

The easiest and least expensive solution is using a small series inductor and integrating the voltage across it but this solution has some drawbacks. The simplest model of an inductor includes an ideal inductor in series with a resistor. The resistor represents the power loss in the inductor. However, the exact model of an inductor is more complicated. Different references have worked on the calculation of inductor parameters (Kassakian, Schlccht & Verghese 1991) (Leon & Semlyen, 1993). A typical realistic model of an inductor is shown in figure 4. C_P is the equivalent capacitance of the inductor. R_L is the serial resistance of inductor winding. R_C is representing eddy current loss and hysteresis loss in the inductor core. L_M is representing magnetizing inductance and L_L is the leakage inductance.

Inductance and resistance variations with temperature and non-ideality of the inductor make this approach nonviable.

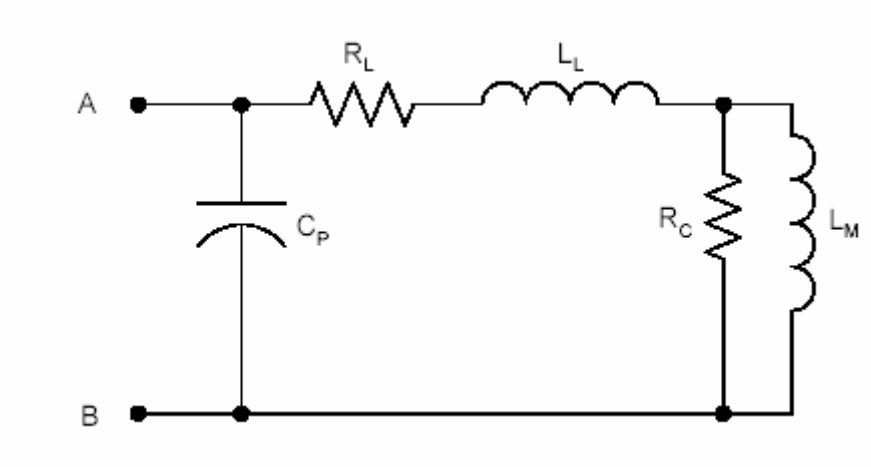

Figure 3.11. A typical non-linear model of an inductor.

The ideal sensor for this purpose is a well-designed current transformer. Proposed current transformer should have very high magnetizing inductance, small leakage capacitance, and linear characteristics over a wide frequency range. Figure 3.12 shows the realistic model of a current transformer. The same as inductor, C_P is the equivalent capacitance, R_1 and R_2 are the winding resistances of primary and secondary, L_1 and L_2 are the leakage inductances of primary and secondary, L_M is the magnetizing inductance, and R_C represents the eddy current and core loss. If we consider that the voltage drop on L_1 and R_1 is not significant, the state space equations of the system are as follows:

$$R_L i_s + L_L \frac{di_s}{dt} + R_L i_s = V_p \tag{3.20}$$

$$i_p = i_{LM} + i_{RC} + i_{CP} + i_S \tag{3.21}$$

$$L_M \frac{di_{L_M}}{dt} = V_P \tag{3.22}$$

$$R_C i_C = V_P \tag{3.23}$$

$$i_{CP} = C_P \frac{dV_p}{dt} \tag{3.24}$$

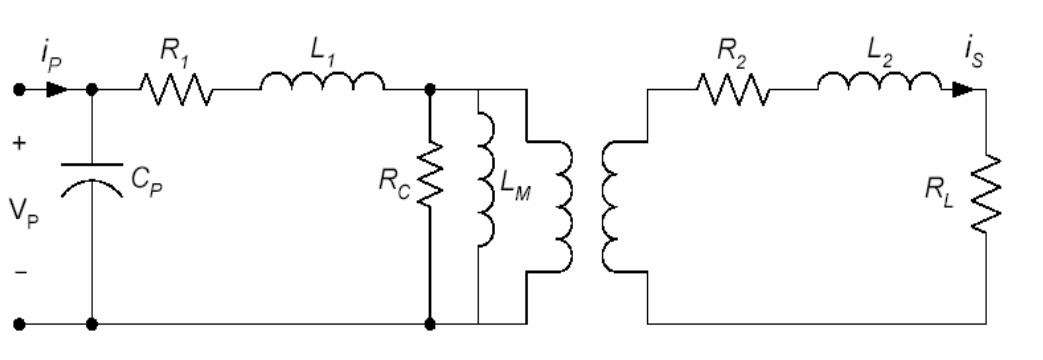

Figure 3.12 A typical non-linear model of a current transformer.

Solving (3.20)-(3.24) using Laplace transform we have

$$i_S = \frac{si_P}{C_P s^3 + As^2 + Bs + C} \tag{3.25}$$

where:

$$A = R_W C_P + R_L C_P + \frac{L_L}{R_C} \tag{3.26}$$

$$B = \frac{R_W + R_L}{R_C} + \frac{L_L}{L_M} + 1 \tag{3.27}$$

$$C = \frac{R_W + R_L}{L_M} \tag{3.28}$$

where R_W is the total winding resistance and L_L is the total leakage inductance. The secondary current is not a linear design, R_W, C_P, and L_L should be minimized and R_C, L_M should be maximized. Optimization of transformer parameters has been addressed in different literature (McNeill, Gupta & Armstong, bt) (Mohr & Bosselmann). The drawback of using current transformers is that they are more suitable for low current application. For high current DC/DC converters, the core size of transformer should be very large.

The third option for current sensor is Rogowski coil sensor. This sensor is suitable for high current application. In this sensor, the primary winding has only one turn

and the secondary winding has multiple turns (Ramboz, 1996). This idea has been used for high power applications for many years. A non-magnetic core is used for the secondary winding, therefore, the sensor has a linear transfer function but its gain is very small. Figure 3.13 shows a typical configuration of a Rogowski coil. The output voltage of the coil can be achieved by:

$$v_o(t) = M \frac{di_P}{dt} \tag{3.29}$$

where i_P is primary current and M is the mutual inductance of primary and secondary windings that can be calculated from:

$$M = n \frac{\mu_0}{2\pi} d \ln \frac{R_a}{R_b} \tag{3.30}$$

n is the number of secondary turns, $R_b = 4\pi 10^{-7}$, and d is the width of the core. Using equations (3.29)-(3.30), value of i_p can be calculated.

3.3.2. Current Injector

An appropriate current injector is needed for configurations shown in figures 3.7 (a) and 3.7 (d). Power electronics switching components such as MOSFET and IGBT are used for power active filters that work in frequencies less than 100 KHz. For controllability of power active filters, the switching frequency of the system should be at least 20 times more than the highest harmonic frequency. The frequency of EMI noises is more than 150 KHz, therefore, no power electronics switching component can be used for this application. Because the power of ripple current is not too much, a MOSFET or BJT based circuit can be used as the current injector. Figure 3.14 shows one type of such an injector. Using of an LM type operational amplifier in the system allows a wide band frequency range as large as 10 MHz. For feed forward amplifier as it is discussed for equation (3.9), the gain magnitude must be close to one. The topology is more sensitive to the phase of the gain. The phase

must be kept very close to zero otherwise the feed forward amplifier deteriorates the ripple compensation. Unlike1 feed forward amplifier, phase of feedback amplifier does not need to be limited. The gain of this amplifier must be designed to have high value.

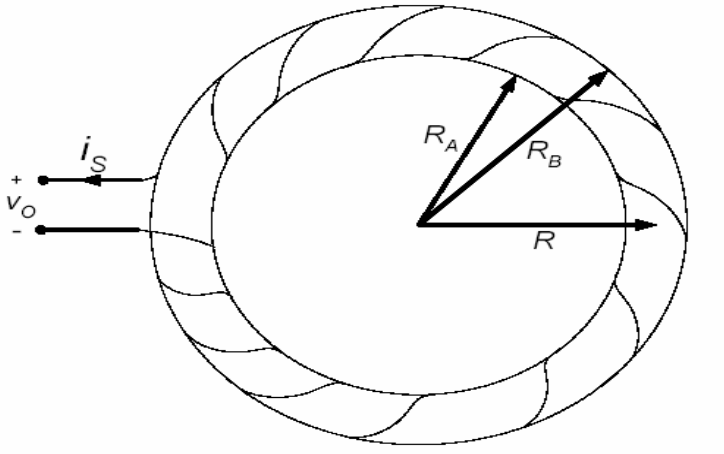

Figure 3.93 A typical configuration of a Rogowski coil.

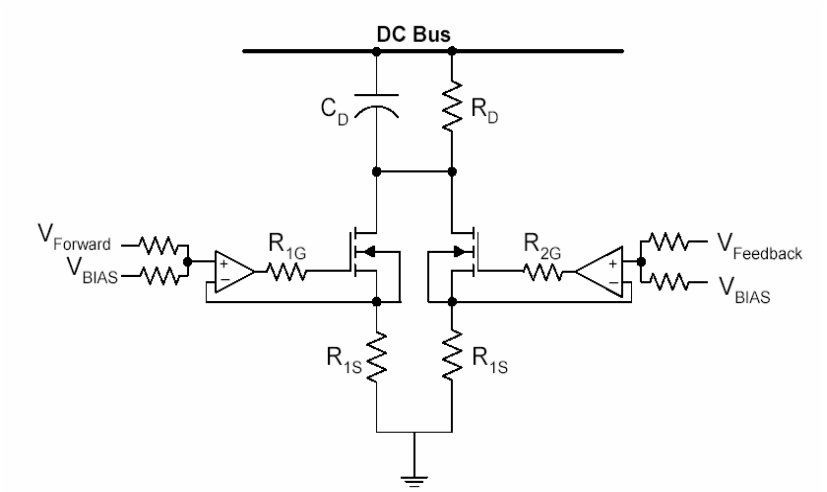

Figure 3.104. A simple type of ripple current injector

In this kind of current injector, the bios current should be at least as high as ripple current to provide complete compensation. All the bios power is being dissipated in the system. Additionally, this kind of current injector dissipates the energy of the ripple current.

3.3.3. Voltage Injectors

Voltage injector in figure 3.7 (b) and 3.7 (c) has more constraints than the current injector. The proposed voltage injector should carry power DC current of the converter. Additionally, it should have wide frequency range. On the other hand, the voltage injector must isolate the control section from the power section. With these features, a high frequency voltage transformer with small magnetizing inductance is a good choice. Figure 3.14 shows a desired voltage injector. DC current of the converter passes through the very small magnetizing inductor of the transformer. Ripple voltage is induced from the primary side by the control circuit. Gain and phase of feed forward and feedback amplifiers must have the same characteristics as current injector.

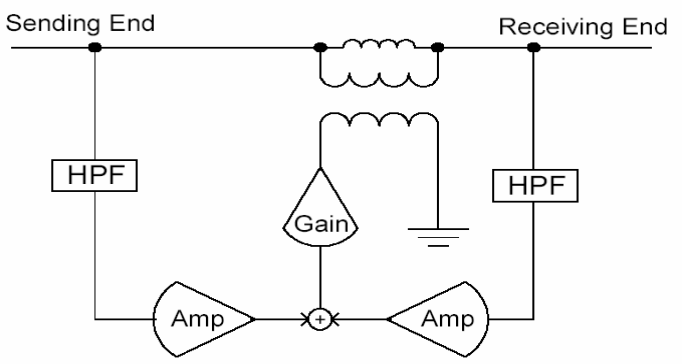

Figure 3.15 A simple type of ripple voltage injector.

CHAPTER FOUR
HYBRID ACTIVE/PASSIVE FILTER DESIGN

During recent years, with the development of power electronic technology, active power filters using high frequency converters have been developed. Compared to conventional dc passive power filter, however, dc active power filter employed on dc side is one of the best effective technique to eliminate current ripple. Recently, active power filters have been proposed and used for ripple reduction in magnet power supplies (Kumagai, Ogawa, Koseki & Nagasaka, 195) (Wang, Joos & Jin, 1997). Whereas, conventional active power filters use transistor banks operating in the linear mode and generate large power losses due to the series dc voltage drop (Hamill, 1996). Because of this, A reactor transformer coupling-type active power filter and transformer-coupled active power filter (Kwon, Suh & Han) in series with a rectifier power supply was adopted. In reference (Liang & Dewan, 1994), a switch-mode ripple regulator (SMRR), works as an active power filter, in series with a rectifier power supply is also proposed.

However, the disadvantage of using a series active power filter is that, the transformer and the high-frequency switches have to conduct the full-load current and the losses of active power filter is high. So that, a shunt-connected active power filter is proposed for the phase-controlled thyristor rectifiers (Wang, Joos & Jin, 1997). In this condition, the high-frequency converter only conduct the small ripple current and the power rating of the dc active power filter is very small.

An alternative to the conventional passive filtering approach is to use a hybrid passive/active filter (Zhu and other, 1999) (Midya & Krein, bt). In this approach, a small passive filter is coupled with an active electronic circuit to attenuate the ripple. The passive filter serves to limit the ripple to a level manageable by the active circuit and attenuate ripple components that fall beyond the bandwidth of the active circuit. The active filter circuit cancels or suppresses the low-frequency ripple components that are most difficult to attenuate with a passive low-pass filter. This approach

permits a substantial reduction in the passive filter size, with potential benefits in converter size, weight, and cost.

If the feedforward gain is K(s), then the transfer function from the ripple source to the output is:

$$\frac{V_{out}(s)}{V_{ripple}(s)} = 1 - K(s) \tag{4.1}$$

A hybrid passive/active ripple filter topology that achieves ripple reduction by injecting an opposing voltage in series with the voltage ripple source is shown in Fig. 4.1. The active circuitry injects a voltage opposing the ripple voltage across the buck capacitor C_{buck} ; thereby reducing the ripple across C_{aul}. The injector design is challenging since it must accurately generate the desired ac injection voltage while carrying the full dc converter current. The injection signal is based on a superposition of easily-measured feed forward and feedback voltage ripple signals.

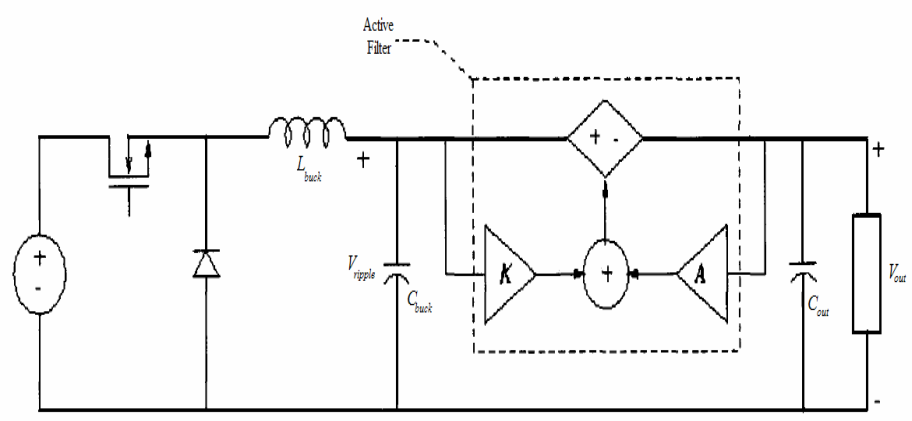

(a)

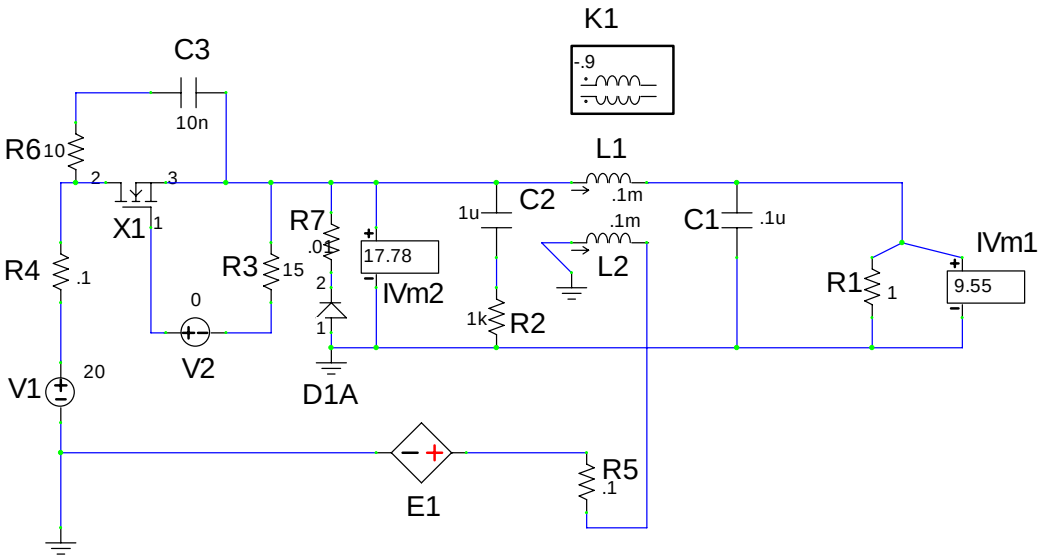

(b)

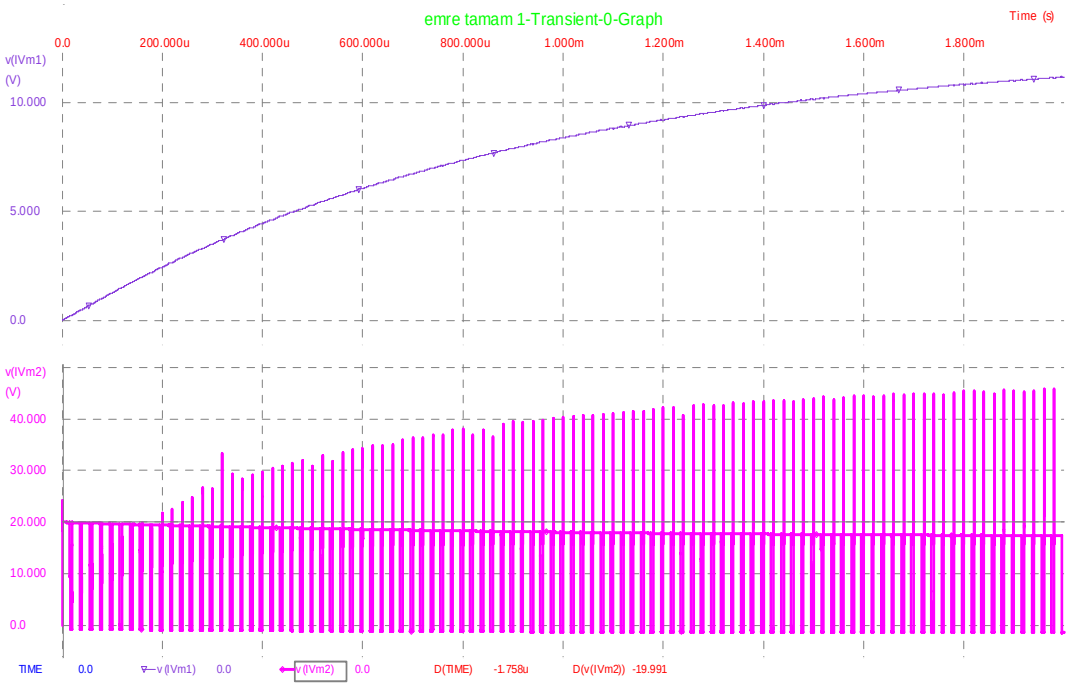

(c)

Figure 4.1.(a) Feedforward / feedback voltage ripple filter used in combination with a passive filter at the output of a buck converter. The hybrid active filter enables a reduction in the size of the passive filter. (b) Pspice similatin model (c) Result of the circuit in figure 4.1.b

For a perfect feedforward path gain of unity, the ripple at the output would be zero. However, due to gain and phase accuracy limitations in the components, feedforward cancellation alone cannot fully attenuate the ripple. Considering the feedback path alone, the ripple source to output transfer function due to feedback becomes:

$$\frac{V_{out}(s)}{V_{ripple}(s)} = \frac{1}{1+A(s)} \tag{4.2}$$

which becomes small as the magnitude of gain A(s) increases. In the feedback case, stability considerations limit the achievable feedback suppression. Combining feedforward and feedback takes best advantage of the injector circuitry and maximizes ripple attenuation. It will be shown that the proposed hybrid passive/active filter structure is attractive in cases where it is desirable to minimize the passive filter capacitance.

The active filter comprises a voltage injector circuit, a control circuit, and voltage sensors. This section considers each of these subsystems in turn.

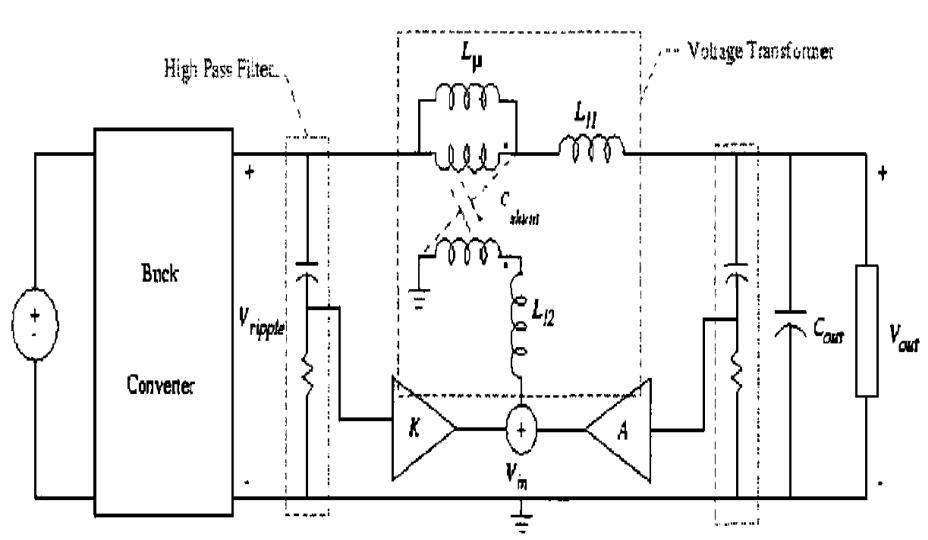

(a)

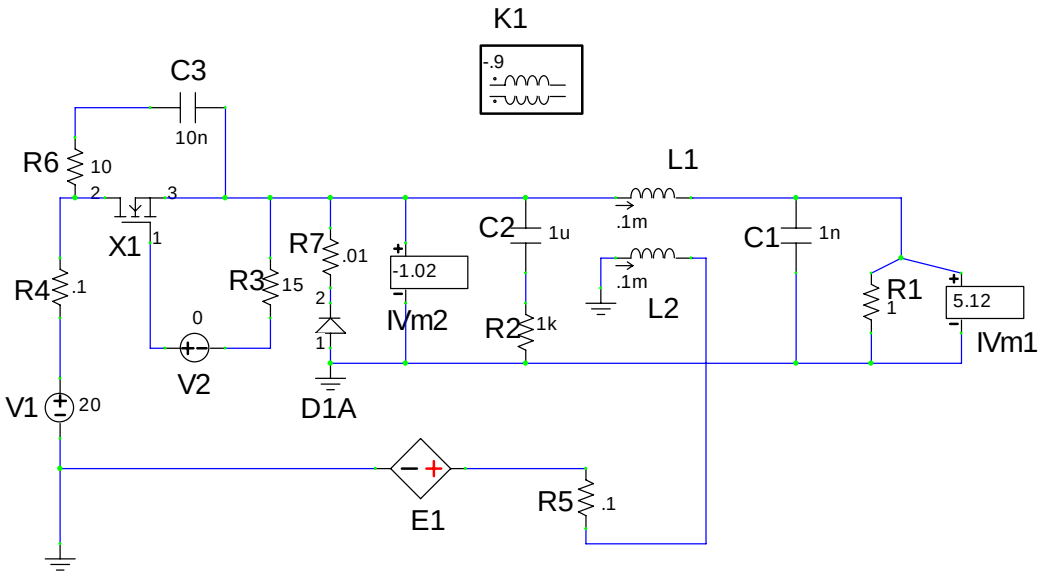

(b)

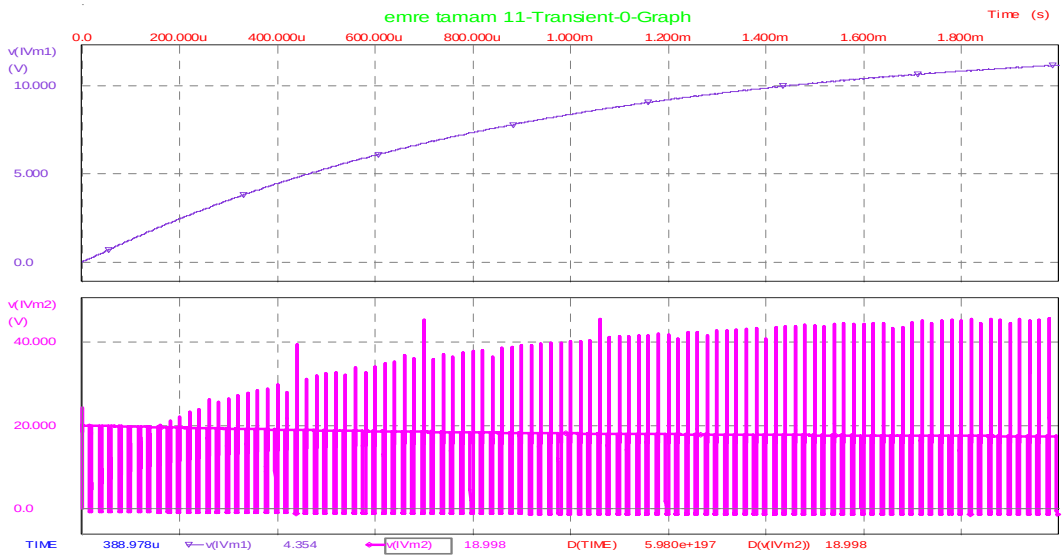

(c)

Figure 4.2 .(a) Implementation of the Hybrid Active/Passive Filter. Voltage is sensed with an op amp via a high pass filter. Voltage is injected using a voltage transformer; the significant transformer parasitics arc shown. L_{μ} is the magnetizing inductance, and L_{11} and L_{12} represent the leakage inductances. (b) Pspice simulation models (c) Result of the circuit 4.2.b.

4.1 Voltage Injector Design

The injector circuit (represented as a controlled voltage source in Fig. 4.1.) must meet a number of challenging requirements. First, the injector must carry the full dc output current with minimal losses. Second, the injector must provide both isolation and sufficient input impedance for the active circuitry. Finally, it must be able to replicate the injector signal with high fidelity.

For the given constraints, a transformer proves to be an ideal choice for a voltage injection mechanism (Feng, Sander & Wilson, 1970). Figure 3.7 illustrates a transformer-based injector, including the relevant transformer parasitics. The dc current of the converter passes through the magnetizing inductance of the transformer, incurring minimal dc losses. The core must be properly sized and gapped to prevent saturation under this heavy bias condition.

The injected, canceling voltage appears across the magnetizing inductance L_μ. The power required to generate this voltage must be supplied by the active circuitry. The transformer magnetizing inductance L_μ and turns ratio must be selected such that the scaled ripple current and voltage can be adequately supplied by the amplifier circuitry. The active circuitry is required to generate an ac voltage of magnitude:

$$V_{circuit} = \frac{N_2}{N_1}\left|V_{ripple}\right| \tag{4.3}$$

and a current of magnitude:

$$I_{circuit} = \frac{N_1}{N_2}\frac{\left|V_{ripple}\right|}{w_{ripple}L_\mu} \tag{4.4}$$

where L_μ is the magnetizing inductance on the transformer's primary side and w_{ripple} is the frequency of the ripple. The magnetizing inductance (and hence transfomer core size) is determined by the output current and dissipation limits of the amplifer circuitry. The transformer turns ratio is used to match the voltage and

current drive levels of the amplifier circuitry to those required for voltage ripple cancellation. To maximize amplifier use and minimize injector size, the turns ratio should be selected to fully utilize the available amplifier voltage and current swing.

For example, the amplifier circuitry in the prototype system has a voltage limit of +/- 7 V, and a current limit of +/-100 mA. To suppress a 2.5 volt peak to peak voltage ripple, a turns ratio of 1:5 is selected. For a 125 KHz fundamental ripple frequency a magnetizing inductance of 5 H.

The use of feedforward ripple cancellation requires that the ripple be both sensed and injected with great accuracy. Therefore the injector must have negligible magnitude attenuation and phase shift for the frequency range of interest; any phase or magnitude error will greatly degrade the performance of the feedforward control. For an ideal transformer, the voltage appearing on the primary side is a perfectly scaled version of the voltage on the secondary side. However, transformer parasitics (Casey, Goldberg & Sclecht, 1988) (Goldberg, Kassakian & Schlect, 1989) (illustrated in Fig. 4.2) can limit the injector performance. Experimental results have verified that C_{shunt} can be neglected, because it does not affect the behavior of the injector for the frequency range of interest. However, the secondary side leakage inductance, L_{12}, forms a voltage divider with the secondary side magnetizing inductance, resulting in a magnitude error. A winding geometry that minimizes leakage inductance is advantageous. After investigating several geometries, while keeping implementation ease in mind, an interleaved primary over secondary winding method was selected for the prototype, as this resulted in a low value of L_{12}.

Stability is a major concern when employing feedback-based ripple attenuation, and is the major factor limiting achievable attenuation. The injector transformer is in the feedback loop, so any phase lag added by the transformer can greatly decrease stability. An ideal transformer adds zero phase lag, but the parasitic inductance on the primary side, L_{11}, plays a surprisingly important role in the stability of the system. The output capacitor, C_{out} form a 2nd order low pass filter, and the phase shift associated with this parasitic filter can affect the stability of the feedback

control. As a result, the transformer design should minimize L_μ to ease the constraints on the control design. A transformer model including parasitics which can cause magnitude and phase errors shown in Fig. 4.3. The leakage inductance is dependent on two factors: winding geometry (as mentioned above) and core gap size. Reducing gap size will reduce the leakage inductance, but it substantially increases transformer size.

The main factors that determine transformer size are magnetizing inductance L_μ maximum allowable flux density B_{max}, gap size, maximum current I_{max} and winding space.

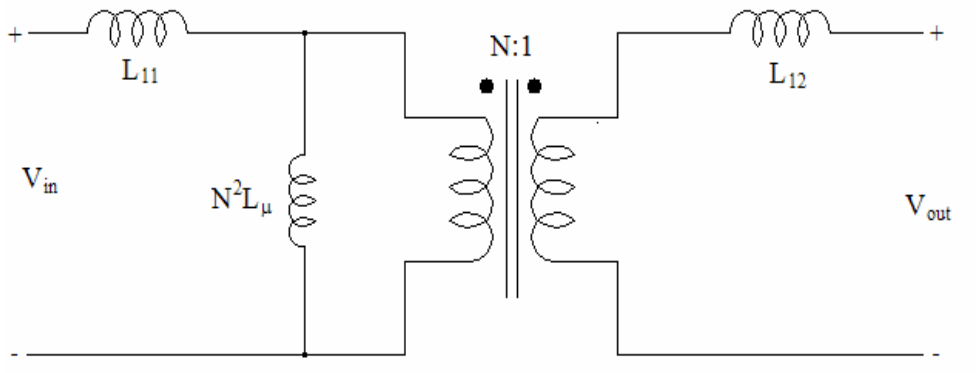

Figure 4.3 A transformer model including parasitics. The parasitics can cause magnitude and phase errors.

The design of the transformer is highly constrained by the particular application. The maximum current is determined by the converter current rating. The magnetizing inductance is set by the active circuitry constraints of equations (4.3) and (4.4). The saturation flux density of the core material B_{sat}, and ac losses determine the maximum allowable flux density B_{max}. For a given current, magnetizing inductance, and maximum allowable flux density, there is a direct relationship between A_L (inductance factor nH/turns^2) and core area, A_{core}:

$$A_{core} = \frac{I_{\max}\sqrt{L_\mu A_L}}{B_{\max}} \tag{4.5}$$

is inversely proportional to the gap size, which typically correlates with leakage inductance. Thus, there is a tradeoff between the leakage inductance and the core size. For instance, the prototype injector could be implemented using an RM10 core but with a relatively large gap. To reduce leakage, the prototype injector is built on a larger RM12 core. This results in a primary side leakage (L_{11}) of 0.156 (O.H (3.4%). The secondary side leakage (L_{I2}) is 23 μH (2.5%). The corresponding attenuation of 9.8 is calculated from eqn.6

$$Attenuation = \frac{N^2 L_\mu}{L_{11} + N^2 L_\mu} = \frac{V_{out}}{V_{in}} \tag{4.6}$$

4.1.1. Alternative Voltage Injector

An alternative method for implementing the injector is to use a bypass inductor in parallel with a high-frequency transformer, as illustrated in Fig. 4.4. In this approach, the bypass inductor, which is implemented with a gapped core and wound with large-gauge wire, serves as the dc bypass element. This function was accomplished by the magnetizing inductance L_μ in the previous case. The high frequency transformer is implemented with a significantly smaller ungapped core with small-gauge wire. This element serves as the means for voltage injection. The relative winding resistances determine the dc current sharing between the inductor and the transformer, while the ac characteristics are determined by the relative inductances. The high-frequency transformer must be implemented with a non-gapped core to keep leakage inductances comparable to the single-core implementation.

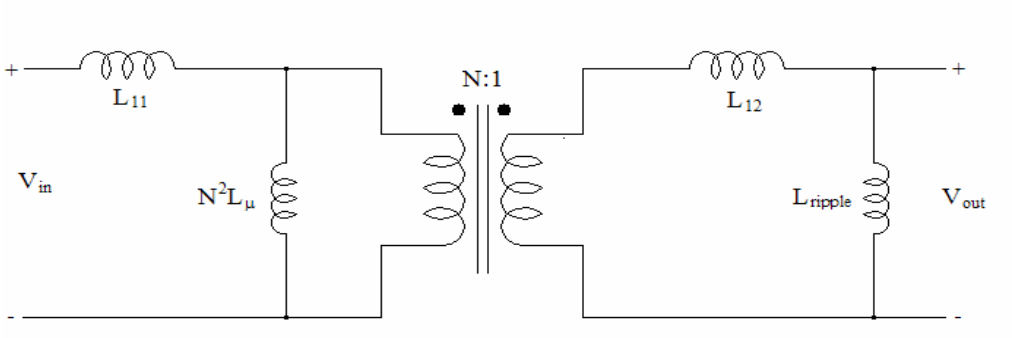

Figure 4.4 Injector implementation uses a bypass inductor in parallel with an high frequency transformer. The significant parasitics are also represented.

The voltage injection attenuation with this approach may be calculated as:

$$Attenuation = \frac{N^2 L_\mu}{L_{12} + N^2 L_\mu}\left(\frac{L_{DC}}{L_{11} + L_{DC}}\right) = \frac{V_{out}}{V_{in}} \tag{4.7}$$

By minimizing the leakage inductances, L_{11} and L_{12}, the attenuation is minimized. It should be noted that in the previous case, only L_{12} caused a magnitude error in the injected signal. In the two-core approach, L_μ also causes a magnitude error, because it forms a voltage divider with the bypass inductor. This approach can thus lead to a larger magnitude error.

CHAPTER FIVE
CONCLUSIONS

This thesis investigated a hybrid passive/active filter topology that achieves ripple reduction by injecting a compensating voltage ripple across a series filter element. The design of sensor, amplifier and injector circuitry suitable for the application is thoroughly studied .

Active ripple filters can substantially attenuate power converter ripple, allowing considerable reduction in passive filter component size. Investigated here is a hybrid passive/active filter topology that achieves ripple reduction by injecting a compensating voltage ripple across a series filter element. Both ripple feedforward and feedback are employed.

The design of sensor, amplifier, and injector circuitry for this application is explored. The simulation results demonstrate the feasibility and high performance of the new approach, and illustrate its potential benefits. It is demonstrated that the proposed approach is most effective in cases where it is desirable to minimize the amount of capacitance in the filtler.

Input and output filters often account for a substantial portion of converter size and cost. Passive LC low-pass filters have been employed to attenuate power converter switching ripple to acceptable levels. An alternative to the conventional approach is the use of an active ripple filter, in which an active electronic circuit (typically coupled with a reduced passive filter) is used to cancel or suppress ripple components at the filter output.

The active filter senses the ripple current in the passive filter inductance and shunts an exact copy of it away from the output capacitance and load. This reduces the ripple seen at the output, and permits a substantially smaller passive filter to be employed than would otherwise be possible. Potential benefits of the active filter approach thus include reduction of the converter size and cost, and improvements in

transient performance. Many types of active ripple filters are possible. Ripple-current filters reduce the ripple current passing through a circuit branch.

Feedforward filters achieve the ripple reduction by measuring a ripple component and injecting its inverse while feedback filters operate to suppress the ripple via high-gain feedback control. Hybrids of these fitler types are also possible, and active filters may be further classified by how the sensing and driving functions are implemented.

This thesis explored the design of feedforward ripple-current active filters. Design of both the current sensor and current injector elements of these filters is considered, and the advantages, limitations, and design tradeoffs of different implementation methods are addressed. The design and simulation evaluation of an active ripple fitler using a novel Rogowski-coil current sensor is treated in detail. This thesis considers the design of current sensors for active ripple filters.

In this tesis, it has been simulated active filter and hybrid active/passive filter, and effect of active filter has been evaluated ripple cancelation.

REFERENCES

A. Goldberg, J.G. Kassakian, and M.F. Schlecht, (1989) "Issues Related to 1-10-MHZ Transformer Design," *IEEE Tran. PowerElectron.,* Vol. 4, No. 1, pp. 113–123.

Bong-Hwan Kwon, Jae-Hak Suh, and Sung-hun Han, (1993) "Novel Transformer Active filters", *IEEE Trans. Industrial Electronics,* vol.40, no.3, pp.385-388.

Cuk, S., Zhang, Z., and Kajouke, L. (1988) "A Low profile, 50W/in3, 500 kHz integrated-magnetics PWM Cuk converter". *In Proceedings of the High Frequency Power Conversion Conference,* San Diego, CA, 442^63.

C. Chow and D. J. Perreault, (2002) "Active emi filters for automotive motor drives," in Proc. *IEEE Power Electronics in Transportation ,* pp. 127-134.

D. Y. Lee and B. H. Cho, (1996) "Design of an Input Filter for Power Factor Correction (pfc) ac to dc Converters Employing an Active Ripple Cancellatio," *in Proc. Energy Conversion Engineering Conference,* pp. 582-586.

David Silber, (1975) "Simplifying the Switching Regulator Input Filter," *Solid-State Power Conversion.*

Dan Sheehan, (1979) "Designing a Regulator's LC Input Filter: 'Ripple' Method Prevents Oscillation Woes,1 Electronic Design 16".

D.C. Hamill (1996) "An Efficient Active Ripple Filter for Use in DC-DC Conversion," *IEEE Trans. Aero, and Electron.* Sys., Vol. 32, No3, pp. 1077-1084.

F. de León and A. Semlyen, (1993) "Time domain modeling of eddy current effects for transformer transients" *IEEE Trans. on Power Delivery,* vol. 8, no. 1, pp. 271-280.

H. J. Boenig, J. A. Ferner, F. Bogdan, R. S. Rumrill, and G. C. Morris, (1996) "Design and operation of a 40-MW highly stabilized power supply". *IEEE Trans. Ind. App.* vol.32, no.5, pp.1146-1157.

*I.*Marneris, R.Bonati, J. Geller, J.N. Sandberg and A. Soukas, (1995) "The Active Filter Voltage Ripple Correction System of the Brookhaven AGS Magnet Power Supply" , *proceeding of the IEEE Particle Accelerator Conference,* V3, P1924-1926.

J. Walker, (1984) "Designing Practical and Effective Active EMI filters," *Proceedings ofPowercon* 11, 1-3 pp. 1-8.

J. Walker, (1984) "Designing Practical and Effective Active EMI filters," *Proceedings of Powercon* 11, 1-3 pp. 1-8.

J. D. Ramboz, (1996) "Machinable Rogowski coil, design, and calibration," *IEEE Transactions on Instrumentation and Measurement,* vol. 45, no. 2, pp. 511-515.

J.G. Kassakian, m. f. Schlccht and g. c. Verghese, (1991) "Principles of Powcr Elcetronics," *Rcading, Mass., Addison-Wesley.*

La White, L.; Schlecht, M.F., (1988) "Design of active ripple filters for power circuits operating in the 1-10 MHz range**"** *IEEE Transactions on Power Electronics Volume* 3, Issue 3, Page(s):310 – 317

La White, L. E, and Schlecht, M. F. (1987) "Active filters for 1-MHz power circuits with strict input/output ripple requirements". *IEEE Transactions on Power Electronics*, 2, 4, 282-290.

L.E. LaWhite and M.F. Schlecht, (1987) "Active Filters for 1 MHz Power Circuits With Strict Input/Output Ripple Requirements," *JEEE Trans. Power Electron.,* Vol. PE-2, No.4, pp. 282-290.

L.R. Casey, A. Goldberg, and M.F. Schlecht, (1988) "Issues Regarding the Capacitance of 1-10 MHz Transformers," *Proc.* IEEE APEC, pp. 352-359.

M. Zhu, D. J. Perreault, v. Caliskan, T. C. Neugebauer, S. Guttowski, and J. G. Kassakian, (2005) "Design and Evaluation of Feedforward Active Ripple Filters," ieee Transactions on Power Electronics, vol. 20, no. 2, pp. 276-285.

M. Zhu, D.J. Perreault, V. Caliskan, T.C. Neugebauer, S. Guttowski, and J.G. Kassakian, (1999) "Design and Evaluation of an Active Ripple Filter with Rogowski-Coil Current Sensing" *IEEE PESCRec.,* Vol. 2, pp. 874 -880 vol.2.

Midya and P.T. Krein, "Feed-forward Active Filter for Output Ripple Cancellation," *Int. J. Elec.,* Vol. 77, No. 5, pp. 805-818.

Nasiri, A.,(2005) "Different topologies of active EMI/ripple filters for automotive DC/DC converters" *Vehicle Power and Propulsion,* 2005 IEEE Conference7-9 Sept. Page(s): 6 pp.

N. McNeill, N. K. Gupta, and w. g. Armstrong,(2004) "Active current transformer circuits for low distortion sensing in switched mode power converters" IEEE Transactions on Power Electronics, vol. 19, no. 4, pp. 908-917.

N.Kumagai,S.Ogawa,S.Koseki,and S.Nagasaka, (1985) "High stability power sources for bending and quadrupole magnets of TRISTAN project", *Hitachi Review,* vol.34, no.3.

N.K. Poon, J.C.P. Liu, C.K. Tse, and M.H Pong, (2000) "Techniques for Input Ripple Current Cancellation: Classification and Implementation," *IEEE T POWER ELECTR*, Vol. 15, No. 6, pp. 1144-1152.

O'Sullivan, D. (1989) “Satellite power system topologies” *ESA Journal,* 13 (1989), 77-88.

P. Midya and P. T. Krein, (1994) “Feed-forward active filter for output ripple cancellation,” *in Proc. IEEE Int. Electron Device Meeting,* vol. 77, no. 5, pp. 805–818.

Rong Liang and Shashi B. Dewan, (1994) "A Low Ripple Power Supply for High-Current Magnet Load" , *IEEE Trans. Ind. App.* vol.30, no.4, pp.1006-1015.

S. Mohr and T. Bosselmann, (2003) “A high dynamic range magnetooptic current transformer with advanced signal processing,” *IEEE Sensors Journal,* vol. 3, no. 6, pp. 744-751.

S. Feng , W. A. Sander, and T. Wilson, (1970) "Small-Capacitance Nondissipative Ripple Filters for DC Supplie," *IEEE Trans. Mag.,* Vol.6, NO. 1, pp. 137-142.

N.K. Poon, J.C.P. Liu, C.K. Tse, and M.H Pong, (2000) "Techniques for Input Ripple Current Cancellation: Classification and Implementation," *IEEE T POWER ELECTR*, Vol. 15, No. 6, pp. 1144-1152.

S. Feng , W. A. Sander, and T. Wilson, (1970) "Small-Capacitance Nondissipative Ripple Filters for DC Supplies," *IEEE Trans. Mag.,* Vol.6, NO. 1, pp. 137-142.

T.K. Phelps and W.S. Tale, (1979) "Optimizing Passive Input Filter Design," *Proceedings of Pwercon 6,* pp. Gl-1 - Gl-10.

T. Farkas and M.F. Schlecht, (1994) "Viability of Active EMI Filters for Utility Applications," *IEEE T POWER ELECTR,* Vol. 9, No. 3, pp. 328-337.

M.S. Moon and B.H. Cho (1996) "Novel Active Ripple Filter for the Solar Array Shunt Switching Unit," *J PROPUL POWER,* Vol. 12, No. 1, pp. 78-82.

Y.Wang, G.Joos and H.Jin, (1997) "DC-Side Shunt-Active Power Filter for Phase-Controlled Magnet-Load Power Supplies." *IEEE Trans. Power Electronics,* vol.12,